3D Real–time Path Planning of UAVs in dynamic environments in the presence of uncertainty

Zammit, C.; van Kampen, E.

Publication date
2021

Document Version
Final published version

Published in
AIAA Scitech 2021 Forum

AIAA SciTech Forum
11–15 & 19–21 January 2021, VIRTUAL EVENT
AIAA Scitech 2021 Forum

10.2514/6.2021-1956

3D real–time path planning of UAVs in dynamic environments in the presence of uncertainty

C. Zammit* and E. van Kampen†
Delft University of Technology, Delft, 2629HS, The Netherlands

Unmanned Aerial Vehicles (UAVs) are being integrated into all spheres of life varying in a wide range of applications from military to civil applications. In such applications, UAVs are expected to operate safely in the presence of uncertainties present in the dynamic environment and the UAV itself. Based on literature different uncertainty sources are identified, quantified and modelled using bounding shapes. The UAV model, path planner parameters and four different complexity scenarios with different moving shapes are defined in view of real UAVs. For analysis uncertainty is varied between 2% and 20% for UAV position and obstacle position and orientation. Results show that both types of uncertainty deteriorate path planning performance of both A* and RRT algorithms for all scenarios considered especially for RRT. RRT results in faster and shorter paths with approximately the same success rate (>95%) as A* for simple scenarios. For complex scenarios A* performs better. This work shows that 3D real—time path planning in different obstacle density, moving obstacle environments in the presence of uncertainty is possible.

I. Introduction

Unmanned or Uninhabited Aerial Vehicles (UAVs), Unmanned Aircraft or more commonly known as drones are defined by International Civil Aviation Organisation (ICAO) as *"pilotless aircraft, in the sense of Article 8 of the Convention on International Civil Aviation, which is flown without a pilot-in-command on-board and is either remotely and fully controlled from another place (ground, another aircraft, space) or programmed and fully autonomous"*.[1] Moreover, Unmanned Aircraft Systems (UAS) extend beyond the aircraft and incorporate all associated elements necessary to operate efficiently and safely an aircraft without a pilot on board.[2]

The idea of UAVs have initiated and progressed concurrently with advances in aviation. In fact, less than 14 years from the first flight of the Wright brothers on 17th December 1903 in North Carolina, on March 1917 A.M. Low launched the unmanned Ruston Proctor AT using compressed air from Salisbury Plain, North England. Over the past 100 years the technology, purposes and use of Unmanned Aerial Vehicles (UAVs) have evolved primarily in view of military demands which have been the main contributor.

UAVs of different sizes and shapes are being integrated into all spheres of life. UAVs are being proposed for a wide range of indoor and outdoor applications varying from surveillance, search and rescue and other military to more civil applications including aerial filming and photography, agriculture, postage delivery and leisure flying. The inclusion of UAVs into the civil airspace and high precision autonomous military applications requires robust autonomous guidance, navigation and control (GNC) systems that shall ensure safe navigation in view of constraints and uncertainties present within manned aircraft and associated supporting systems, UAV systems and the environment in which they will operate. Oppositely to UAVs which were economically viable for the mainstream only over the last decade, manned aircraft systems have been in civil operation for quite some time. As a result, Standard Operating Procedures (SOPs) for both fixed and rotary wing manned aircraft are well defined mainly as a result of post-incident analysis. In fact, although UAV manufacturers are pushing for integration as the commercial prospect is unbounded, ICAO is cautious

*Ph. D. Candidate, Control & Simulation, TU Delft Aerospace Engineering, Kluyverweg 1, Delft, The Netherlands and AIAA Member
†Assistant Professor, Control & Simulation, TU Delft Aerospace Engineering, Kluyverweg 1, Delft, The Netherlands and AIAA Member.

and is only foreseeing a medium-term integration of remotely-controlled UAVs within non-segregated and aerodrome environments. Moreover, ICAO[2] indicates that fully autonomous UAVs will not be integrated within civil aviation systems in the foreseeable future.

One fundamental difference between a machine and a human is that the latter is accustomed to deal efficiently with uncertainty from early childhood improving his/her skills through adequate training while programming machines to deal with uncertainty in real time is not straight forward. Although certain constraints such as buildings, no–fly zones and particular kinematic constraints can be defined accurately, in reality the absolute majority can only be defined with an element of uncertainty, for example weather, fuel consumption and vehicles' position and state. Furthermore, constraints can pop–up whilst in flight and the path planning algorithm shall be able to mitigate these *a priori* unknown situations.[3]

Uncertainty in path planning has been investigated for quite some time. In the beginning uncertainty was considered as a domain of complaint control and uncertainty was mitigated by allowing or requiring the agent to touch.[4] Although contact with an obstacle can be accepted for gripping or manipulators, in UAV path planning applications this must be avoided at all costs.[4] However, different researchers stress about the need for robust and generic path planning solutions that can be applied in the presence of uncertainty. Dadkhah *et. al.* points out that while efficient algorithms offering solutions to sub–problem exist, general real–time path planning solutions in the presence of uncertainty is still pending.[5] Similarly, Goerzen *et. al.* remarks that more research is required to deal with different uncertainty sources as till now this field has not been adequately studied.[4] Furthermore, Vanegas *et. al.* identified the need for a model and a system that can incorporate sensing uncertainties in the UAV state calculation besides uncertainty in target location.[6]

These researchers and others outline the need to investigate the effect of uncertainty in path planning of UAVs both for indoor and outdoor environment. This motivation is key to the definition of the aim of this paper. Therefore the aim of this paper is to investigate the effect of uncertainty on the performance of real–time 3D UAV path planning in a dynamic environment. For the scope of this study the two most utilised path planning algorithms in the graph–based and sampling–based categories will be assessed namely the A* and the Rapidly–Exploring Random Trees (RRT) algorithms. It will be assumed that the planner has no *a priori* knowledge of obstacle paths and/or future positions. Moreover, the uncertainty if any of different parameters is not provided to the planner at initiation stage and it can change while the UAV is constructing and traversing the path in real–time. For real–time path planning, the planner must generate the path in at least the time required by the UAV to traverse it.[7–9] The path length, computational time and success rate will be the performance measures that will be considered to assess the performance of the A* and RRT algorithms in a 3D real–time environment. The dynamic environments developed in our previous work[10] will be considered.

The paper will be organised as follows. Section II will present the state-of-the-art in path planning of UAVs in the presence of uncertainty. Section III provides a brief resume of the A* and RRT algorithms, the smoothing algorithm which is only applied to the RRT algorithm, the real–time path planning platform and the dynamic obstacle definition framework all extensively described in our previous works.[10–13] Section IV will define the environmental scenarios, the UAV model and path planner parameters definitions and constraints and uncertainty modelling and quantification rationale in view of 3D real–time path planning algorithm. Section V will present and analyse the results in view of real–time 3D UAV path planning requirements. This paper will conclude with Section VI highlighting the main outcomes, strongholds and shortcomings of this study whilst pointing out future recommendations.

II. Path planning in the Presence of Uncertainty Review

A. Introduction

This section will first identify the need for path planning in the presence of uncertainty. Then a list of different uncertainty sources and their challenges to the path planning problem will be explained. The following section will deal with the representation and quantification of uncertainties proposed by different studies. This section will conclude with a resume of the performance of different path planning algorithms in the presence of uncertainty. This will help identify the strongholds and shortcomings of each method independently and in relation to others.

B. The need for path planning in the presence of uncertainty

Everything in this World is uncertain although uncertainty can be quantified to a certain degree. Therefore in an indoor or outdoor environment a UAV path planning system will have to deal with a number of factors some of whom incorporate different uncertainties. These include partially known environments, limited payload capacity, limited on-board computational power, differential constraints, environmental disturbances and uncertainty in both state and measurement.[5] Path planning in unknown or partially known environments it is commonly assumed that unknown space is occupied.[24]

An effective path planner in the presence of uncertainty must *always* guarantee that the UAV will reach and stop at the goal region without colliding with any obstacle despite uncertainty in sensing and control.[19] To achieve this, the planner must simultaneously consider the projected motion of obstacles and the time–varying uncertainty in their location.[27] In addition UAV state uncertainty including both perception and dynamics shall also be considered.[16,21]

Different studies tried to incorporate uncertainty modelling within their path planning systems. Although as will be discussed in the next sub–sections different approaches have been made to eliminate or heavily attenuate uncertainty effects on path planning systems Kim *et. al.* remarks that path planners that require global or extensive local information may not guarantee satisfactory performance in the presence of uncertainty.[14] Therefore, the issue of uncertainty in sensing and control cannot be neglected in real UAV applications.[4] Goerzen *et. al.* remarks that uncertainty and robustness has not been fully studied. This study considers these two fundamental aspects as paramount in determining the prospect of an algorithm that must be efficient, optimal and robust at the same time.

Cui *et. al.* considers UAV dynamic path planning as extremely challenging due to different uncertainties, magnitude fuzzy and interaction of these factors and constraints present within UAV utilisation environments.[16] The planner has to deal with errors and imperfections of sensing systems to figure out threats and positional, kinematics and dynamics information for state estimation in real–time. Moreover, UAV mission objectives and control modes of operation of UAVs further add to the complexity of the problem.[16]

C. Uncertainty Sources

Different uncertainty sources were considered in different studies. LaValle *et. al* segmented uncertainty in robotic systems into 4 categories namely: uncertainty in robot sensing, uncertainty in robot predictability, uncertainty in environment sensing and uncertainty in environment predictability.[17] This imply that uncertainty sources are derived from the sensing and prediction derived as well from the sensing of the agent and the environment in which the agent resides. The same rationale can be applied to 3D UAV environments. In this study, uncertainty sources are segmented into 4 main categories: UAV model, UAV sensing system, environmental sensing and prediction and communication uncertainties:

1. *Uncertainty in Sensing System*
   - Generic sensor errors;[18,19]
   - Uncertainty in pose information both of UAV and target;[5,16,21–23]
   - Uncertainty in localisation, velocity and acceleration of both UAV and the target;[4,16,19,20,24,25]
   - Initial uncertainty state.[16,20,21]
2. *Uncertainty in UAV model*
   - Uncertainty in system modelling including agent dynamics;[5,26]
   - Disturbances from the nominal model;[18]
   - Uncertainty in system configuration sensing;[21,26]
   - Uncertainty in command tracking precision;[4,5]
   - Estimation Uncertainty;[24]
   - Uncertainty in the system error distribution.[16]

3. Uncertainty in Environment Sensing and Prediction

- Uncertainty in environmental situational awareness such as obstacle locations and threats;[4,5,19,25,26]
- Uncertainty in future environment prediction;[26–28]
- External disturbances into the operational environment example wind, atmospheric turbulence and rain.[5,6,19]

4. Uncertainty in Communication

- Communication errors, delays, packet dropouts,and finite communication ranges.[18]

D. Uncertainty Modelling

The uncertainty sources described in the previous section need to be mathematically modelled for the path planning algorithm to reach the target successfully. As the guidance, navigation and control systems can be designed as modular sub–systems, modularity can also be applied to segregate and individually define uncertainty sources even based on mission requirement.[5] The uncertainty modelling strategy will have a direct influence on the robustness of the path planning system. Uncertainty modelling can be broadly categorised into two main categories: Bounded Shapes and Probabilistic Distributions.[24,29]

1. Bounded Shapes

Bounded shapes consider worst–case bounds to define the edges of the bounding shape.[24] Bounded shapes were used to define both threats and obstacles but also state definitions. With reference to the latter, robustness in the presence of uncertainty can be ensured by attentively adjusting the safety margin between failure and nominal states.[26] Bounded uncertainties in state estimation and disturbances were modelled in[30,31] to verify non linear UAV models. Results show elegant formulations of verifiable planning.[30,32] Chance–constraint optimisation is a method used for path planning in the presence of uncertainty.[33,34] This method upper bounds the probability of collision at any time instant by a constraint in the optimisation process.[24]

Bounded uncertainty can be modelled as time variant and time invariant. In fact, Page *et. al.*[35] modelled an extroceptive sensor that allowed a bounded time invariant uncertainty in its sensing zone. Another study developed the use of "safe zones" that reset to zero or quasi–zero the uncertainty bounds until the agent remains in the safe zone.[36] In this case, uncertainty can be time variant as long as the extrapolation of uncertainties is limited by visiting safe zones. Similarly, Larson *et. al.*[37] defined a 2D time variant obstacle area to simulate in real–time obstacle dynamic properties including change in speed and direction in unmanned surface vehicles.

Different shapes were considered to estimate uncertainties. Lihua *et. al.*[25] estimated GPS position by a cylindrical region centred at the agent position with radius and height equal to the horizontal and vertical position estimation accuracy. Yang *et. al.*[38] mitigated control and sensing uncertainties by modelling obstacles as ellipsoids in 2D and a ball shaped regions in 3D. Similarly, ellipsoids were used to model uncertainty of intermediate points used in the construction of the path to the final goal while a bounding box is defined around the vehicle to provide a safety margin for uncertainties in the vehicle position.[21] This time variant bounding box is inflated by a multiple of the standard deviation as uncertainty propagates during path following.[21] The rate of inflation depends upon the distance from the origin (which is assumed to be known with certainty) and the visual scale as the latter determines the quality of the position estimate.[21] Also, ellipsoids were used by Pepy *et. al.*[39] to model state distribution uncertainty of robot position and orientation at the configuration.

2. Probabilistic Distributions

Uncertainty in this category define a specific or a set of unbounded distribution functions to estimate uncertainty for different parameters or agent states.[24,30,32] Robustness in probabilistic estimations will limit the failure probability depending on the definition of distributions.[26] Van der Berg *et. al.*[40] modelled obstacle uncertainty using a Linear–Quadratic–Gaussian (LQG). Positional uncertainty was also modelled with an independent Gaussian distribution in.[41] In this study, fixed obstacles were modelled using a constant

measurement uncertainty. For quasi–static obstacles the centre of position remains at the initial location while for moving obstacles at constant speed the centres will move accordingly.[41] For both quasi–static and moving obstacles the positional uncertainty will grow linearly with time as long as the obstacles are not continuously observed.[41,42] Florence[24] considers only continuous depth information in the local frame of reference for robustness in the presence of uncertainty in state estimation.

A normal distribution around the mean take–off position was used in[6] to account for initial uncertainty. A bounded normal distribution with mean about the desired heading was considered in the same study to mitigate with motion uncertainty. Similarly, Wen *et. al.*[43] estimated the standard deviation of the probabilistic UAV state distributions at each tree node by Linear Quadratic Gaussian Motion Planning (LQG–MP). Uncertainty in threats were estimated by bounded circles with different risk factors. These studies showed that hybrid approaches are also an option that can be considered.[43]

E. Uncertainty Quantification and Reduction

Different research works considered different time invariant and time variant uncertainty values for different parameters independently and concurrently. These are linked with other mission, environmental and UAV modelling constraints. This section provides a resume of a sample of implementations with the associated uncertainty values. Rathbun *et. al.*[27] limited speed between 21m/s and 34m/s, turn radius to a minimum of 0.18km and 1.52 times the fuel necessary to travel the distance from the initial position to goal. In the same work, the authors concurrently considered a bounded obstacle positional uncertainty of 0.1km, a bounded uncertainty for velocity of 5km/s and an uncertainty growth of 0.001km/s/s. Similarly, Cui *et. al.*[16] considered a variable speed UAV with predefined bounds (10m/s to 50m/s) and initial speed of 25m/s in an obstacle free environment. Concurrently the authors considered an initial distance error of 30m, 30m and 2m, respectively in all dimensions, a horizontal velocity error of 2m/s, an angle error of 0.5^o and 10% distance and 0.2% angle uncertainties in the system error distribution. Other works considered a predefined holistic uncertainty. In this regard, Yang *et. al.*[38] considered a bounded control uncertainty of 0.5m. As regards to obstacle size quantification Zeng *et. al.*[41] represented each obstacle by a circle with a radius of $2\times$ the standard deviation implying a confidence interval of 95.4%.

From the implementations described in this section it is shown that uncertainties in different parameters are defined at initiation stage propagating at predetermined rate as the mission progresses. Some researchers have identified ways how such uncertainty can be reduced. One way is by detecting using sensory vision systems identification tags placed on static non-enemy obstacles. As these are fixed sensory errors can be reset.[20] Others make use of previous information to attenuate uncertainty in already visited areas.[6] Another solution is to shorten the path planning time reducing uncertainty increase at an expense of reducing the path planning success and optimality and/or making the path planning solution more complex to compute.[6] Another approach is to consider only the latest sensory measurement data with the scope of reducing time propagated uncertainty.[44–46]

F. Path planning solutions under uncertainty

Researchers have implemented a number of path planning solutions to mitigate with uncertainties in different parameters. The following will outline the different path planning methods that were proposed.

1. Rapidly–Exploring Random Tree (RRT)

The RRT algorithm is one of the most utilised path planning algorithms in the presence of uncertainty. Although this method has been successful implemented to plan in complex real world scenarios such as autonomous driving such as in the DARPA challenge,[47] this algorithm does not explicitly incorporate uncertainty.[26] This inherent characteristic has encouraged researchers to apply the RRT algorithm in uncertain environments by adding uncertainty into the planned paths.[48–50]

In this regard, the chance constraint RRT, an RRT variant, was developed and employed to handle uncertainty in model and environmental situational awareness in different implementations.[24,34] This method is implemented to achieve robustness against uncertainties by growing trees of state distributions. However this method requires an accurate vehicle dynamics model to grow a tree of state distributions.[26]

Another variant was developed by Yang *et. al.*[38] In this work the authors added a guiding attraction factor to the RRT variant, RRT* to enhance path convergence and smoothness in less computational time in

the presence of fixed obstacles with uncertainty in both 2D and 3D environments. Auode *et. al.*[51] remarked that RRT–based estimators offer both accuracy and efficiency for long–term prediction of dynamic threats in uncertain and partially unknown environments.

In another approach, Kothari *et. al.*[26] generated probabilistically robust paths in partially known environments using the RRT algorithm. Kothari *et. al.*[26] stresses about the need to modify the RRT algorithm to an anytime algorithm to arrive to a real time solution. The authors remark that based on the results the computational time increases approximately linearly with the number of obstacles.

The Dynamic Domain Rapidly–Exploring Random Tree (DDRRT) combined with a linear Quadratic Gaussian Motion Planning (LQG–MP) use developed by Wen *et. al.*[43] to plan paths under threats and uncertainties. Static threats incorporating uncertainty were modelled using intuitionistic fuzzy sets while dynamic threats were modelled using the pursuit–evasion method. The path was further enhanced by the safety adjustment method and the RRT* a variant of RRT. Results show that this system was able to construct online safe paths in uncertain and hostile environments.

Finally, Achtelik *et. al.*[21] made use of the Rapidly–Exploring Random Belief trees to evaluate offline multiple path hypothesis in a known map with fixed obstacles so as to select a path exhibiting the motion required to estimate vehicle state. The planner consequently selects paths that minimise uncertainty state estimation in the estimated states without neglecting kinematic and dynamic model constraints. Also due to the sampling based nature of this approach no assumptions on discontinuities in measurement uncertainty with respect to vehicle position are considered. Results show that this approach improves the precision of state estimation and that a naive planner will not be able to generate a successful path in an environment with bounded uncertainty in most cases. Furthermore, it was noted that uncertainty is close to null at the start, increasing during straight sections and when leaving feature–rich areas and decreasing at the goal provided a perfectly working re–localisation system. Results show that the scaling factor of the monocular vision–based system, that requires excitation, was fundamental to maintain the uncertainty within bounds whilst the UAV flew away from the origin. In this regard, authors remark that uncertainty bounding boxes need to be significantly enlarged when crossing unknown areas with uncertainty scale reducing in non direct paths while remaining unchanged for direct paths.

2. A Algorithm*

The use of the A* path planner to plan in the presence of uncertainty is not frequently used when compared to RRT and its variants. However this does not imply that this graph–based method is unsuitable to operate in an uncertain environment. In this regard, Liao *et. al.*[19] developed a 3D, A* based, closed–loop path planning algorithm for VTOL UAVs in GPS–denied, obstacle–rich environments. This algorithm provides collision–free shortest path from the current UAV position to any final goal point. The authors remark that this method is implicitly robust to uncertainty mainly due to the closed–loop approach.

3. Markov Decision Processes (MDP) and Partially Observable Markov Decision Process (POMDP)

The MDP algorithms generate policies that allow the agent to formulate a series of actions to maximise return or cost functions without neglecting uncertainties.[52] MDP assume that states are completely observable while POMDPs incorporate uncertainties in sensing and partial observability of the agent.[53,54] Vanegas *et. al.*[20] developed an on–line POMDP algorithm that relies only on on–board localisation sensors to generate UAV control actions in the presence of uncertainty. To improve the quality of the control actions the POMDP algorithm is allowed to calculate for longer times although this will increase the uncertainty in motion due to longer prediction time.[6]

4. Sliding Mode Control

Sliding mode control has inherent benefits that makes it a potential candidate for mobile robotics. Such benefits include robustness against system uncertainties, good dynamic response and stability under large disturbances.[55] Robustness against different uncertainties such as matched uncertainty in nonlinear system is achieved by the sliding mode algorithm's systematic approach.[56]

5. Linear Methods

Linear algorithms can handle disturbances system control and model uncertainties and therefore can be used for path planning under uncertainty. These algorithms can describe the environment completely while modelling kinematic and dynamic constraints.[57] In this regard, Mixed Integer Linear Programming (MILP) methods merge binary and integer logical constraints to model the system and environment.[57–59] Optimal control can be used to find a path based on a set of differential equations.[60] This method can be regarded as a variant of linear methods. In optimal control methods there exist a infinite number of variables' states as opposed to linear approaches. Using linear chance constraints to model uncertainties in optimal methods makes the method more computational efficient.[57]

6. Reactive Path Planning Methods

Reactive path planning strategies are also potential candidates that can be employed to mitigate uncertainty in real–time. This approach use only local knowledge of obstacles and threats to plan without generating a global plan either offline or at the initiation stage.[5] Reactive path planning systems make use of either vision–based or depth sensor–based systems to constantly update the path planning algorithm with real–time environmental information. For better reactiveness to uncertainties or changing environmental situation, feedback controllers can be employed. Reducing the complexity of feedback controllers can enhance robustness.[4]

7. Potential Fields and Probabilistic Maps

Potential fields assign a potential function to free space with the agent reacting to forces due to repelling potential from obstacles with the goal node having the lowest potential.[4] A Laplacian potential field method was developed by Connolly[61] with the scope of minimising collisions with obstacle fields during random movement. Similarly, Lazanas *et. al.*[62] considered potential fields to navigate through regions but with no uncertainty. Oppositely, Lihua *et. al.*[25] developed the Modified Artificial Potential Field (MAPF) to navigate through an uncertain environment with randomly moving obstacles and pop–up threats. Obstacles are modelled by non–isotropic spatial volume creating repulsion potential fields. Results for test carried out at 5km altitude and maximum speed of 60m/s show an improvement over the standard Artificial Potential Field approach.[25]

In the same category as potential fields are probabilistic maps that define defines the exposure to threats as a function of location and time. The undeterminisitic nature of dynamic environments has motivated Zengin *et. al.*[63] to develop such a probabilistic map any apply it to the problem of dynamic path planning. The authors use state–space search to approach the goal location while avoiding threats.

8. Other methods

Path planning in dynamic environments with uncertainty are too complex for classical approaches to guarantee a solution. These algorithms tend to be inefficient and may lock in local minima without producing non–optimal paths.[4]

Simultaneous Localisation and Mapping (SLAM) is important in situations of path planning under uncertainty, although it does not directly address the planning phase.[4] This method is able to provide localisation information and hence attenuate the level of uncertainty. SLAM has been used for real–time laser mapping in a remotely controlled helicopter flight[64] and to provide situational awareness under uncertainty in real–time in the DARPA Grand Challenge.[65]

Receding Horizon Control (RHC) can also be employed for path planning under uncertainty. Goerzen *et. al.*[4] remarks that an online RHC framework can modify an offline generated path to handle in flight uncertainties that are either unknown or partially known at the initiation stage. In this regard, Kuwata *et. al.*[66] used the RHC method to generate trajectories for an agent under the influence of atmospheric turbulence.

Q–learning is an optimisation method used to deal with uncertainties. Cui *et. al.*[16] modelled uncertainties to control the acceleration and bank angle of a UAV using tracking error cost function optimised through Q–learning in a 2D environment without obstacles.

Shell Space Decomposition (SSD) scheme is a method that decomposes the environment into concentric shells radiating out from the start to the goal location with single or multiple control point in each shell

region.[41] Zeng *et. al.*[41] applied SSD with a quantum–behaved particle swarm optimisation path planner for an Autonomous Underwater Vehicle (AUV) with static, quasi–static and moving obstacles in a cluttered and uncertain environment. Paths are generated offline and results show a better performance with concentric circles and sphere algorithms.[41]

Finally, in another approach, Schouwenaars *et. al.*[67] developed a robust system that accounts for uncertainty in manoeuvring of vehicles. This system is based on a control architecture developed by Frazzoli.[68] This control system is based on the quantization of system dynamics to reduce computational complexity of motion planning in nonlinear, high dimension environment.

G. Conclusion

This section highlighted the need to consider uncertainty during path planning especially in dynamic environments. The different uncertainty sources considered in various works were categorised into 4 main categories. The two main uncertainty modelling methods namely bounded shapes and probabilistic distributions were explained based on their applications in different environments with different obstacles and threats. Another subsection presented a resume of parametric quantification of uncertainty in different working environments. Also this part highlights how different authors tried to reduce uncertainty or its effects. Finally, the different path planning methods that were used in different works not only for UAVs are presented and the resulting outcomes analysed and compared. This review helps in defining a path planning strategy for an agent operating within an environment with the respective kinematic and dynamic constraints and uncertainties.

III. A*, RRT, Smoothing and Real–time Algorithms

A. Introduction

This section will initiate with a brief definition of the two most utilised graph–based and sampling–based algorithms, namely the A* and RRT algorithms. The smoothing algorithm developed to mitigate the non–optimality of the RRT algorithm will then be explained. Finally, this section will conclude with a summary of the A* and RRT real–time path planning implementations.

B. The A* algorithm

Graph–based methods define the state space into an occupancy grid defining obstacles residing in grid points as unavailable points. Graph–based algorithms check the possibility of a path between start and goal position using only obstacle–free grid points.[69] Graph–based algorithms only offer a guarantee of solution if an appropriate resolution is selected.[70]

The standard A* algorithm uses a heuristic evaluation function ($f(n)$) to determine the cost of neighbouring grid points.[71] This evaluation function sums the cost from the current position to a prospective future position and the cost from the latter to its goal node.[71,72] For a detailed explanation of this algorithm refer to our previous work.[11–13]

C. The Rapidly–Exploring Random Tree (RRT) Algorithm

Sampling–based algorithms construct a path between start and goal positions by connecting unevenly selected obstacle–free points in the configuration space.[70,73] Opposite to graph–based methods, these algorithms offer a guarantee of solution within an infinite time as opposed to graph–based methods provided that a path exists.[70]

The standard Rapidly–Exploring Random Tree (RRT) constructs a unidirectional tree by randomly planting seeds in obstacle–free points. A new tree branch is constructed by selecting a new point a predefined distance from the nearest tree node on the line interconnecting the latter node with the randomly selected point, provided that the line from the nearest tree node and the new node is obstacle–free. A path from start to goal points is formed when one tree branch reaches the goal provided the first tree node is the start position.[74–76] The RRT algorithm is efficient in complex high–dimensional environments but lacks optimality and requires smoothing.[76–78] Just as for the A* algorithm, a more detailed explanation of the RRT algorithm and its variants is provided our previous works.[11–13]

D. The Smoothing Algorithm

The path generated by both A* and RRT algorithms is constructed by interconnecting path points. The developed smoothing algorithm randomly selects two of these path points and then randomly defines two points on the path segments connecting the initially selected path points with their respective next path points. If the interconnection of the latter two points is obstacle–free then all path points in between are neglected, creating a shorter path with lesser turns and lesser path points. This process is repeated until the percentage path length reduction over the last 20 iterations is less than 1% and for a minimum of 20 iterations. A more detailed explanation of this algorithm is provided in our previous works.[12,13]

This post–path construction smoothing algorithm was developed to mitigate with the non–optimality characteristics of the RRT algorithm. Since in our previous works,[11,12] the A* algorithm produced the shortest possible path with the considered resolution, improvement with the smoothing algorithm was only marginal. Moreover, in a real–time A* implementation some parts of a smoothed, obstacle–free path which are very near to obstacles, can produce collisions as the graph points can shift due to discretisation in the next intermediate path construction as the UAV current position moves. Therefore, this smoothing algorithm was only applied for the RRT algorithms.

E. The Real–time Algorithm

Literature identifies the need for real–time path planning if the UAV is expected to travel in dynamic environments especially if the environment is partially unknown or totally unknown except for a limited Field of View (FOV) at the initiation stage.[79–81] Owing that the scope of this work is to design a path planning algorithm for such scenarios, an algorithm to emulate real-time behaviour was developed in a previous paper.[13]

The developed real–time path planning algorithm selects an obstacle–free intermediate goal node in the direction of the final goal position a look-ahead distance from the current UAV position. This look–ahead distance is governed by the sensory system's FOV. Consequently, a path from the current UAV position to the intermediate goal node is constructed (if possible) using either the A* or RRT algorithms depending on which algorithm is being examined. The UAV current position travels along the intermediate path a predetermined distance determined from the UAV speed and maximum allocated intermediate time. It is assumed that actuator systems' response is modelled with high fidelity with no uncertainty and the UAV is not effected by external factors. Furthermore it is assumed that during UAV travelling the environment remains static. This assumption is valid since a low intermediate time is considered. A no solution situation exists when either a no intermediate obstacle–free path was not constructed in the allocated time and/or the total time to reach the goal from the initial position has exceeded. The various UAV parameter definitions defined in our previous work,[13] are briefly explained in Section IV C. For a more detailed explanation of the described real–time algorithm and performance results for both path planning algorithms, refer to our previous work.[13]

F. Conclusion

This section briefly described the two most utilised graph–based and sampling–based methods, i.e. the A* and RRT algorithms. To mitigate the non–optimality of the RRT algorithm a smoothing algorithm was also developed. The real–time algorithm made up of either the A* or RRT with the smoothing algorithm provided a test platform to assess the performance of both configurations in view of real life UAV applications.

IV. Environmental scenarios, UAV model and path planner parameter definitions and constraints and Uncertainty Modelling and Quantification

A. Introduction

This section will describe how uncertainty factors are integrated within the environmental and UAV model frameworks. This section will initiate with a description of the modelled environmental scenarios. Then the UAV model and path planner's parameter constraints will described. Bounded uncertainty is then defined for size and obstacle positions while randomised but bounded uncertainty is considered for UAV positions. In the final subsection, the percentage uncertainty bound values applied to both obstacles and UAV position are described.

B. Environmental Scenarios

Four different scenarios with different complexities developed in our previous work[10] are considered as a test platform to assess the performance of the A* and RRT algorithms. These time variant environments are generated offline with an associated time stamp prior the initiation of path planning. Cubes, V shaped obstacles and 2D planes with window openings are used in the development of these obstacle scenarios. The cubes and V obstacles are randomly placed in the environment with each point having the same probability of occupancy. The following list describe the construction of each of the four scenarios, namely:

- Scenario 1. 10 cubes of 0.1x0.1x0.1 with no rotation;
- Scenario 2. 10 cubes the same size as Scenario 1 but with random rotation at definition stage and with changing independent rotation with time iterates;
- Scenario 3. 10 V obstacles constructed by adjoining one side of each of the two planes with an angle of 53° between the planes. Each plane has a size of 0.1x0.112 and is randomly rotated as in Scenario 2. This plane size was considered so that it fits exactly into the considered cube; and
- Scenario 4. Two planes on the Y–Z axis separated by 0.4 each with a window of 0.2x0.2 as well as the obstacles in Scenarios 2 and 3 combined.

Figure 1 illustrates pictorially each scenario for a random time iterate without considering any uncertainty bounds. Since moving obstacles are considered, the positions of each obstacle for each scenario will change in every time iterate.

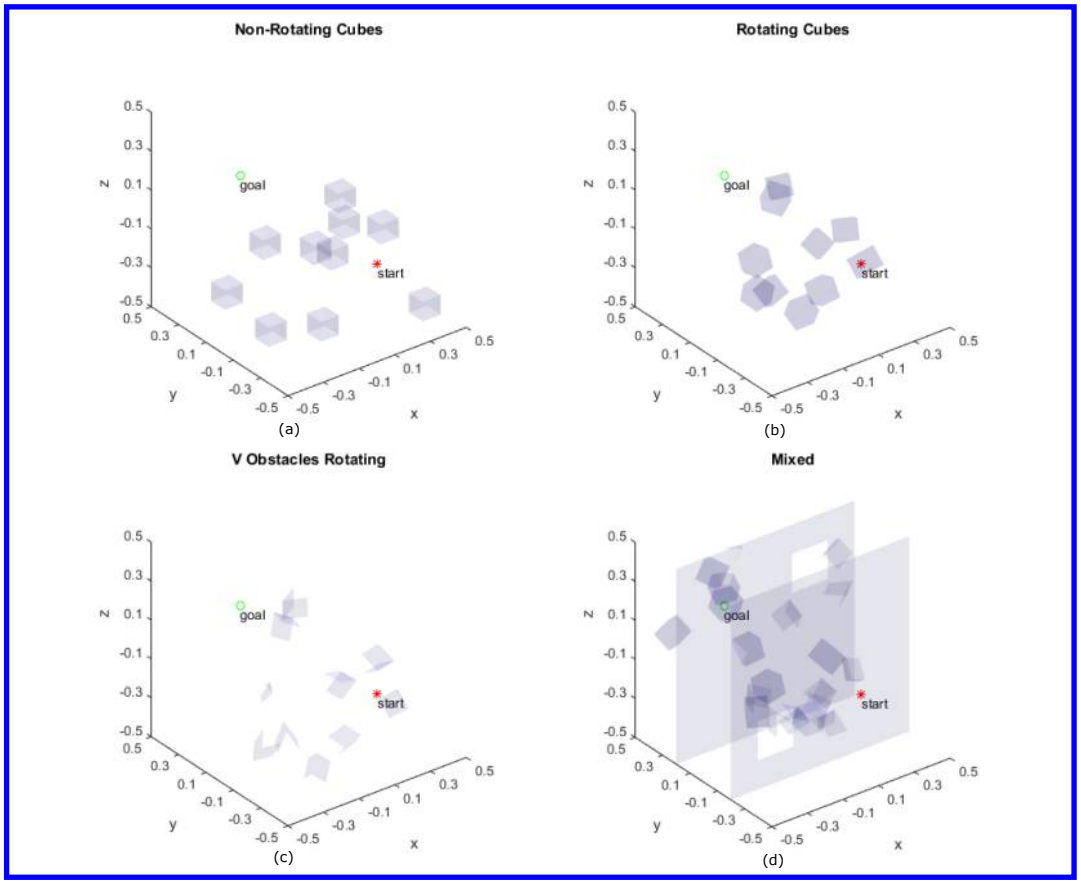

Figure 1. Environmental scenarios: (a) Non-rotating cubes scenario, (b) Rotating cube scenarios, (c) V obstacle rotating scenario and (d) Mixed scenario. These scenarios incorporate cubes, V obstacles and obstacle planes in the Y-Z with windows as openings.

Table 1. Obstacle shapes

Shape	Size	Number of Planes	Closed/Open
Cube	0.1x0.1x0.1	6	Closed
V obstacle	0.1x0.112	2; (53^o with each other)	Open
Plane with window	1x1	1; window (0.2x0.2)	Open

C. UAV model and path planner parameter definitions and constraints

To fairly assess the performance of both path planners, nominal UAV and path planner parameter values tabulated in Table 2 and adapted from our previous work[13] are derived after considering real UAV model characteristics, features and constraints.

Table 2. Real–time algorithm parameter definition

Parameter	Nominal Value	Units
Resolution (res)	21	[-]
Step size RRT (d_{step_RRT})	$\frac{1}{21-1} = 0.05$	[-]
Distance to travel per iterate (d_{s_step})	$\frac{2}{res-1} = 0.1$	[-]
Distance between current UAV position and prospective new intermediate goal point (d_{int_goal})	0.4 and 0.6 for Mixed case scenario	[-]
Maximum time to generate path segment ($t_{iterate\_max}$)	$\frac{d_{s\_step} \times 60 \times 60}{100 \times v_{UAV}}$	s
Maximum time to generate path ($t_{path\_gen\_max}$)	$10 \times t_{iterate\_max}$	s
Distance reduction factor (d_{factor})	0.8	[-]

A cube of 1x1x1 was considered as the environmental space, with fixed start and goal points at (0,-0.5,0) and (0,0.5,0), respectively for all considered tests. For A* algorithm the environment and start and goal points were shifted by a random distance between 0 and half the distance between grid points to eliminate path length ripple as thoroughly explained in.[12]

The resolution, considered for graph–based methods such as the A* is defined as the number of grid positions per dimension. Oppositely in sampling–based methods all obstacle–free space is available for path construction. Therefore, the tree branch length set as the distance between grid positions in A*, was considered for RRT to offer a fair comparison between the two methods. The distance to travel per iterate (d_{s_step}) is set at double the distance between grid positions and tree branch length while the distance between the current UAV position and an intermediate goal point (d_{int_goal}) is set to double d_{s_step}. For the mixed case, d_{int_goal} is increased from 0.4 to 0.6 since the planner need to be able to visualise the second plane window to construct a path to the intermediate goal point that may result on final goal side of the second plane. If this distance is not increased the window will not reside within the FOV of the planner and consequently a no solution situation will result. All these parameters were set based on performance analysis in our previous work.[13] The maximum time to generate a path segment ($t_{iterate\_max}$) was defined as the time needed for the UAV to travel d_{s_step} while the maximum time to generate the whole path ($t_{path\_gen\_max}$) was set at 10 times $t_{iterate\_max}$. Finally, the distance reduction factor is used to reduce the distance in cases where prospective intermediate goal points or prospective UAV positions reside on an obstacle. Again this parameter was empirically defined after performance analysis in our previous work.[13]

For each test situation the UAV speed remained constant. This parameter was varied between 0.01[-]/s and 0.1[-]/s in steps of 0.01[-]/s, where [-] represent modular distance units. These values were determined based on the nominal speeds for exploration situations in a nominal environment. The environmental time stamped space created *apriori*, assumed that obstacles move in random directions with random speeds smaller than the UAV speed.

D. Bounded Uncertainty Definitions

In the literature review presented in Section II, uncertainty was divided into four main categories, namely uncertainty in sensing systems, UAV model, environment and communication. The first three categories of uncertainties aforementioned will effect position and orientation of the UAV and obstacles within the FOV of the UAV sensing systems. Therefore, by modelling probabilistic and/or bounded uncertainties in position and orientation of the UAV agent and obstacles, uncertainties in sensing systems, UAV model and environment will be catered for. Owing that our UAV is assumed to be stand–alone no communication is exchanged with other third parties and therefore communication uncertainties is out of scope for the purpose of this work. Furthermore, since in this work it is assumed that the UAV is a point model, orientation uncertainty is also neglected.

After considering both bounded and probabilistic uncertainty modelling methods, bounded uncertainty was considered to model uncertainty in both obstacles and UAV position. As described in literature, both methods were successfully applied to model different kinds of uncertainty in all four categories described earlier. The real–time path planning algorithms are designed to consider any point in the environmental space as either unoccupied or occupied by an obstacle, implying that the latter point is either free or unavailable. With probabilistic methods, each point has a probability based in the distribution function of either being free or unavailable and therefore the planner must define *apriori* or in real–time a threshold to assign such point as free or unavailable. This will increase computational demand with respect to the bounded shape method which only defines a bound around the obstacle or UAV position and assumes that within the bound, parameters are known with certainty and outside the bound everything is totally unknown. Therefore through this rationale the latter method was selected.

Figure 2 illustrates the bounded boxes around the different obstacle shapes and the spherical bound around UAV position. 3D bounded boxes were considered since obstacle shapes can be regarded as 2D squarish planes. Therefore, 3D bounded boxes are shapes that offer equidistant bounds from the actual obstacle limits. A spherical bound was considered for UAV position estimation as for fair modelling the uncertainty error must be equidistant in all directions for the estimated UAV position point. In this work, we will assume that uncertainty is time invariant in both obstacle position and orientation and UAV maximum deviation in position since we will assume that within the look–ahead distance, the sensing accuracy and precision of the UAV sensing systems and the UAV positional accuracy system are assumed to remain constant. Having said this, the effect on performance by varying uncertainty will be analysed in Section V.

The actual UAV position in real–time path planning is assumed to reside with equal probability anywhere within the spherical bounds defined by the time invariant maximum deviation in position. Therefore for the scope of analysis, the current UAV position is randomly selected within the spherical bounds of the estimated future UAV position on the constructed path in the previous iterate. This randomisation process is repeated in the construction of each path segment while each scenario with a specific speed is repeated for 100 times.

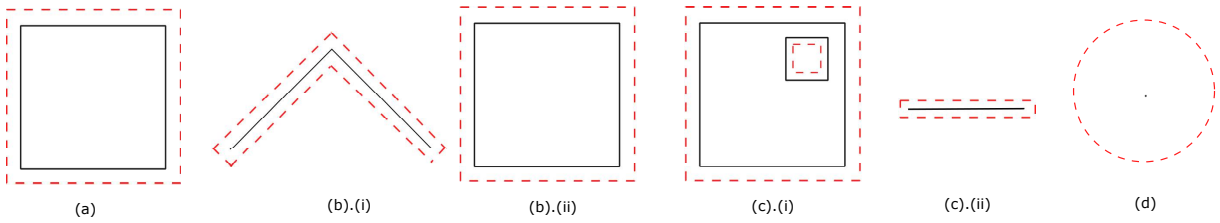

Figure 2. 2D illustrations of uncertainty bounds for all three categories of 3D obstacle shapes and the UAV position: (a) Cube (bounds are applied the same for all cube sides), (b) V–obstacle, (c) Planes in the Y-Z with windows as openings and (d) UAV position

E. Uncertainty Quantification

Uncertainty in obstacle position and orientation is governed by either the precision and accuracy of the on–board UAV sensing systems only or by on–board sensing systems fused with other ground or associate off-ground sensing systems. In both cases, environmental situational awareness is limited and provided to the path planner with a degree of accuracy and precision depending upon the sensing capabilities of the aforementioned system or systems.

The uncertainty bounds of 3D obstacles namely cubes are quantified as a percentage of the volume of each obstacle. Therefore, the cube increases in volume by the percentage uncertainty. For the V–obstacle case, which is made of two 2D planes perpendicular to each other, uncertainty bounds are quantified by 10 planes enclosing the V–obstacle from all sides as illustrated in Figure 2. The percentage uncertainty factor in obstacle position is multiplied by the distance between the centre of the shape and each node of the obstacle and then added to the actual node position to identify the nodes of the 10 enclosing planes such that the distance between any node on the V–obstacle planes and the respective bound limit is equidistant. For the mixed case, incorporating all shapes including 2D planes with windows, the uncertainty bound for planes is constructed by using two other parallel planes with smaller windows with the edges of the parallel planes connected with each other to form a closed shape as illustrated in Figure 2.

The nominal uncertainty percentage values of obstacle shapes are decided based on the uncertainty quantification considered in different studies and presented in Section II. E. As regards, obstacle uncertainty three studies were presented one that considered probabilistic and the others considered bounded uncertainty. Yang *et. al.*,[38] considered a constant circular and spherical uncertainty bound of an additional 0.5m radii for 5m radii obstacles for 2D and 3D environments, respectively. This amounts to 10% uncertainty bounds. Rathbun *et. al.*,[27] considered a 0.1km positional uncertainty for obstacle aircraft which amounts to 2x the size of a medium sized passenger aircraft. This environment is different from the environment under review since in this case the size of obstacles and obstacle density is much larger with respect to the environmental space than Rathbun *et. al.* study and thus only Yang *et. al.*[38] is considered for the definition of uncertainty bounds for obstacles.

The maximum uncertainty in UAV position is modelled as a sphere as illustrated in Figure 2 (d). The radius of the sphere is equal to the multiplication of the respective uncertainty and the distance the UAV moves per iterate d_{s_step}. Cui *et. al.*,[16] considered a 10% distance and 0.2% angle uncertainty in system error distribution in an obstacle free scenario. The selected spherical uncertainty bound will be larger with respect to Cui *et. al.*[16] for the considered speed since 0.2% angle uncertainty will translate to approximately 1.3% lateral deviation and in our case we are assuming a maximum deviation of 20%. This allows a safer navigation and/or by using less accurate and precise positioning systems.

For all considered scenarios the uncertainty in either obstacle position and/or UAV position was varied between 2% and 20% in steps of 2% when the effect of this uncertainty on performance is under review. Otherwise, it is assumed that uncertainty is neglected.

F. Conclusion

This section presents the four different environmental scenarios with different difficulties that are used to assess the effect on path planning performance in real–time in the presence of time invariant uncertainty in both obstacle position and orientation as well as UAV position using bounded shapes. The considered uncertainty factors and their quantification incorporate a set of major uncertainty sources although other uncertainty factors neglected in this study may negatively impact performance of the considered path planning algorithms in real–time.

V. Results

A. Introduction

The A* and RRT 3D real–time path planning algorithms, environmental scenarios and uncertainty in UAV and obstacle position and obstacle orientation described in the previous sections were implemented in MATLAB and tested using an Intel Xeon ES–1650, 3.2GHz. The path length, computational time and success rate are the performance measures considered. Unless uncertainty is under review, UAV speed is varied in steps of 0.01[-]/s, starting from 0.01[-]/s to 0.1[-]/s as described in Section IV, otherwise the UAV speed is set at 0.05[-]/s. Section IV.C while the parameters tabulated in Table 2 were assigned to the nominal values.

B. A* and RRT with no uncertainty

Prior the inclusion of uncertainty in obstacle and UAV positions, the performance of both the A* and RRT algorithms in real–time in the presence of moving obstacles is assessed. This is important so as to compare the effect on performance of uncertainty additions to both A* and RRT. Figure 3 adapted from[10] show the

path length, computational time and success rate for A* and RRT as speed is varied between 0.01[-]/s to 0.1[-]/s for the constant parameters illustrated in Table 2.

The salient points that can be concluded from Figure 3 is that the path length for the first three scenarios namely the cube with no rotation, the cube with rotation and the V–obstacle produce a path very close to 1 for all scenarios for all speed for both algorithms. The shortest path length is recorded for the cube with no rotation followed by the cube with rotation and the V–obstacle also for all speeds for both algorithms. The straight line distance from start to goal is 1 implying that the planner only deviated by a small percentage from the straight line owing that the obstacles are rarely in the line of sight from start to goal. A major increase in path length is recorded for both A* and RRT for all speed as the planner needs to traverse through two planes with windows on opposite sides as illustrated in Figure 1. Overall the path length for RRT was shorter than A* for all scenarios and all speeds considered. Also speed has no effect on path length since speed only determines the maximum intermediate and total time allocation.

The computational time for A* is longer than that for RRT for all scenarios for all speed. As for path length speed has no effect on computational time for both algorithms for the reason described previously. The V–obstacle resulted in the lowest computational time followed by the cube without and with rotation for both algorithms with a major increase for the Mixed case. This order is attributed to the computational difficulty associated with each scenario with the V–obstacle consisting of only two 2D planes while cubes consist of 6 planes and the internally unavailable space. For both path length and computational time A* results in higher variance with respect to RRT for all scenarios for all speeds. This is attributed to the graph–based nature of the A* algorithm and the ripple reduction algorithm that re–plan the environment each iteration. Refer to[10, 12] for further details.

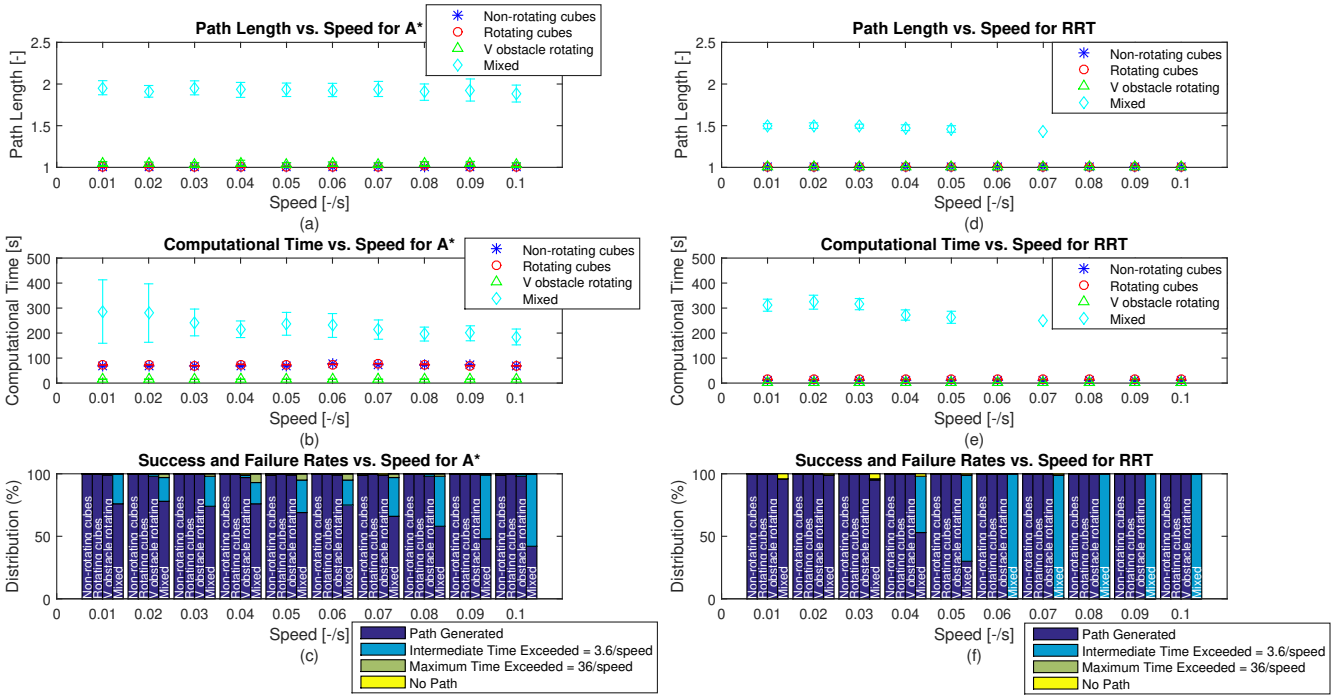

Figure 3. Performance parameters vs. speed: (a) Path Length for A*, (b) Computational Time for A*, (c) Success and Failure rates for A*, (d) Path Length for RRT, (e) Computational Time for RRT and (f) Success and Failure rates for RRT for 100 iterates for each considered situation (speed and scenario) with 95% confidence interval. ($res = 21, d_{s\_step} = 0.05, d_{int\_goal} = 0.4$ (for Scenarios 1,2 and 3) and $d_{int\_goal} = 0.6$ (for Scenario 4), $d_{factor} = 0.8$ and $t_{iterate\_max}, t_{path\_gen\_max}$ are a function of the UAV speed) Adapted from[10]

In terms of success rate both algorithms exhibit a near 100% success rate for the first three scenarios with RRT exhibiting a 100% success rate for the mentioned scenarios for all speeds while A* achieved a minimum of 95% success rate for the same set of scenarios. For the Mixed case, the RRT achieved a success rate of a minimum of 95% for speeds from 0.01[-]/s to 0.03[-]/s deteriorating to 0% as speed increases. The A* on the other hand never achieved this high success rate of the RRT algorithm but maintained success rate above 40% at the highest speed which is the worst case scenario. For further analysis of these results

refer to.[10]

Overall the performance of both the A* and RRT algorithms show that they can be applied to real–time path planning in the presence of moving obstacles as long as the allocated intermediate and total time is appropriate. The next step is to include uncertainty in UAV position as explained in Section IV.

C. A* and RRT with uncertainty in UAV position

The inclusion of uncertainty in UAV position is factored as a percentage of the distance that the UAV is expected to move per iterate which is predetermined. During planning the path is expected not reside less than this distance away from each obstacle. Figure 4 illustrates the performance response of the A* and RRT algorithms with uncertainty in UAV position. In this test two inter–related parameters are changing concurrently. One is the maximum uncertainty in UAV position that dictates the safe distance that the planner must keep to ensure a non-collision provided the obstacle remains fixed. Secondly, when the UAV is simulated to traverse the path in real-time, a random shift by a random distance in a random angle varying from 0 to the considered maximum UAV positional uncertainty is added to the calculation of the next intermediate UAV position on the previously constructed path to the intermediate goal point. This random distance is bounded between 0 and the maximum uncertainty defined in the x–axis of Figure 4.

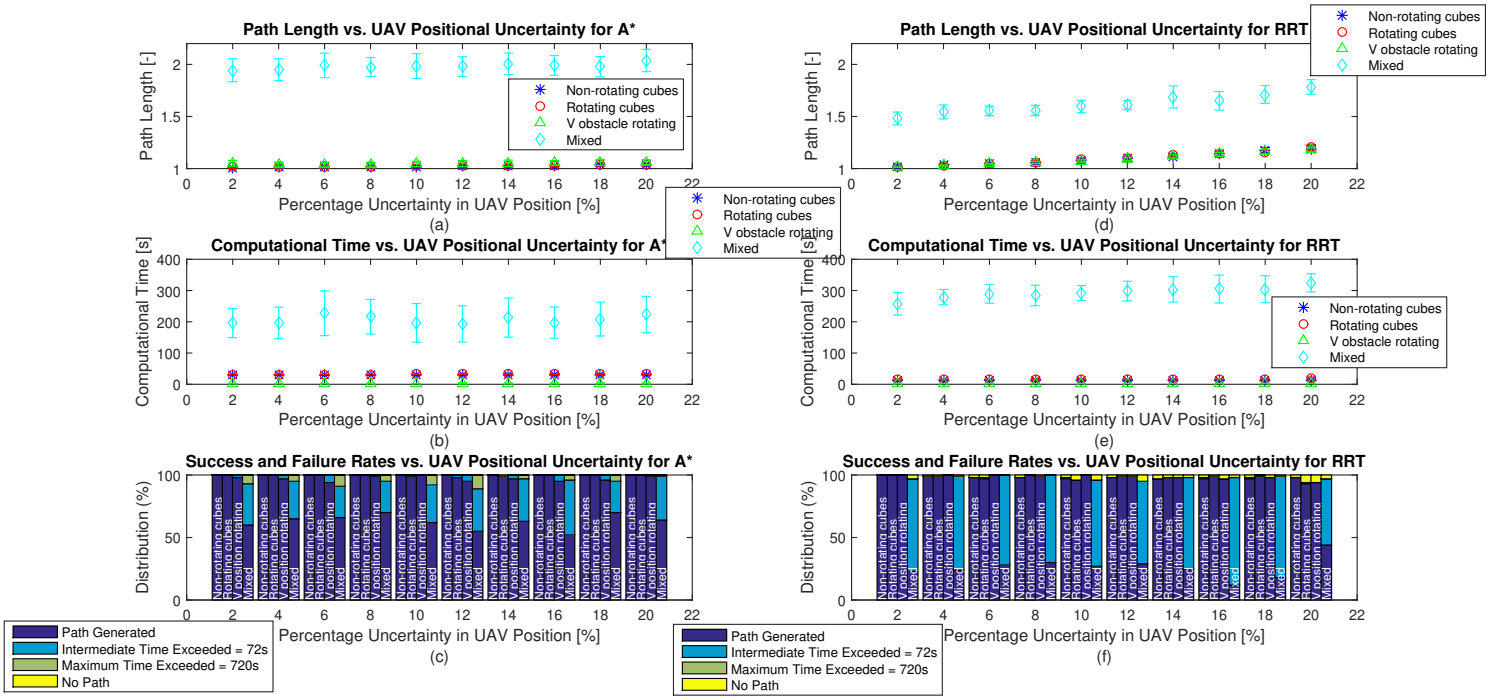

Figure 4. Performance parameters vs. Uncertainty in UAV position: (a) Path Length for A*, (b) Computational Time for A*, (c) Success and Failure rates for A*, (d) Path Length for RRT, (e) Computational Time for RRT and (f) Success and Failure rates for RRT for 100 iterates for each considered situation (obstacle uncertainty and scenario) with 95% confidence interval. ($res = 21, d_{s\_step} = 0.05, d_{int\_goal} = 0.4$ **(for Scenarios 1,2 and 3) and** $d_{int\_goal} = 0.6$ **(for Scenario 4),** $d_{factor} = 0.8$**,** $t_{iterate\_max} = 72s$ **and** $t_{path\_gen\_max} = 720s$**.**

The mean shortest path length for A* results is recorded for the non-rotating cube case increasing when rotation is introduced and increasing further in the V-obstacle and Mixed cases. For RRT, the V-obstacle is the shortest followed by the cube without and with rotation and the mixed scenario, although the difference in the first three scenarios is small. This order is equivalent for the no uncertainty cases for A* but changes with RRT mainly that the V–obstacle experienced the largest deterioration. The V-obstacle rotating case is made up of two planes with each one having an area greater than each side of the cube. Due to the buffer distance the available volume between planes is reduced and therefore the planner need pass from outside in a larger number of iterations, resulting in a longer path.As for the non uncertainty cases, it can be concluded that rotation increases path length since the effective movement of the cube is higher by introducing rotation effectively requiring the UAV to travel further away to avoid collisions.

The path length for the first three scenarios is 2 times and 1.5 times longer for the Mixed case with respect to the other cases for all speeds for the A* and RRT algorithms, respectively. As for the no uncertainty cases this increase results since the planner need to travel through obstacle plane windows on opposite sides of two parallel planes spaced by 0.4[-] from each other. Due to the graph–based nature of A* obstacles are defined with a buffer of half the distance between grid positions while for RRT every point not on an obstacle plane or within the object is accessible.

The mean path length for RRT is 7.4%, 6.9%, 4.0% longer and 18.4% shorter with respect to A* for Scenarios 1 to 4, respectively. For Scenarios 1 to 3 the success rate is close to 100% for both algorithms therefore a fair comparison can be made but for the Mixed case A* exhibited a higher success rate that could effect the mean path length owing that the easiest iterates (which are ultimately successful) are considered for RRT with more difficult iterates besides the easiest ones are considered for A*. This is also applicable to computational time analysis. Therefore, without uncertainty the path length recorded for RRT was always smaller than that for A*. So with the inclusion of UAV positional uncertainty both algorithm experienced an increase in path length with the major deterioration exhibited by the RRT algorithm. In fact, with the inclusion of uncertainty, A* exhibited a mean increase of 1.8%, 1.7% and 1.2% and a decrease of 2.7% for Scenarios 1 to 4, respectively for the same speed. A larger increase of 9.2%, 9.1%, 8.9% and 10.7% is recorded for RRT for Scenarios 1 to 4, respectively for the same speed. The decrease in path length for A* for the Mixed case is attributed to the lower success rate for A* for this case and therefore the easiest iterates are considered as explained earlier.

Further analysis of Figures 4 (a) and (d) show that for both algorithms for all scenarios the path length increases with percentage uncertainty in UAV position. For A* the path length increases from 2.7%, 2.8%, 1.2% and 4.8% for Scenarios 1 to 4, respectively for uncertainty increases from 2% to 20%. A similar analysis for RRT shows that the path length increases by 16.7%, 18.2%, 16.7% and 20.4% for Scenarios 1 to 4, respectively. From this analysis, the comparison between the mean path length of A* and RRT and the comparison between the A* and RRT with and without uncertainties, it can be concluded that both algorithms experience an increase in path length with uncertainty and the RRT is more susceptible to increase in uncertainty in UAV position with respect to A*. For A* a buffer distance in obstacle definition is already considered even without uncertainty at half the distance between grid positions which is equal to 0.05[-] for the considered resolution. Therefore, with the inclusion of an uncertainty buffer from obstacle and a deviation from the projected position due to the added uncertainty in position, the A* planner will already incorporate a buffer space minimising the effects of uncertainty as opposed to RRT which besides the positional uncertainty would not include any buffers between the UAV prospective path and obstacles. The major percentage path length increase is recorded for the Mixed case since it incorporates more than double the paths, restricting the construction of intermediate paths.

Computational time is lowest for the V-obstacle case for both algorithms for all range of uncertainties considered since the planner need to only check for collision with only two planes per shape not six planes and their interior per shape as in the cube case. As described for other situations rotation increases computational time as the effective movement of the obstacle increases. Since the mixed case is more complex than the other three cases the required computational time is higher as a consequence.

With the inclusion of uncertainty A* recorded a decease in mean computational time by 2.29 times, 2.29 times, 5.60 times and 3.7% for Scenarios 1 to 4, respectively for the same speed. Oppositely, for RRT an increase of 16.3%, 8.9%, 13.1% and 11.6% is recorded for Scenarios 1 to 4, respectively for the same speed. The decrease exhibited for A* results since, with uncertainty, the planner keeps a larger distance from the obstacles and therefore the chance of re–planning due to obstacle movement decreases while the obstacle definition time and path planning remains the same. This reduces computational time at the expense of longer path length. For RRT a smaller increase in computational time results with increase in uncertainty. By increasing uncertainty in RRT, tree branches are more restricted and therefore the planner requires more time to construct the path although as for A* the re–planning time reduces. But since the path construction time is greater than the re–planning time, the combined effect is that the total computational time increases.

The mean computational time for A* is 2.43, 2.04 and 1.13 times longer and 29.6% shorter with respect to RRT for Scenarios 1 to 4, respectively. As for the non-uncertainty case, for both algorithms, the shortest computational time is recorded for the V–obstacle case followed by the cube without rotation and with rotation and the Mixed cases. Although, without and with uncertainty A* reduced and RRT increased in computational time, this difference is not enough for the A* to perform better than RRT in the first three scenarios. Also, results confirm that for complex cases, the A* can construct a path in less time than RRT

with and without positional uncertainty. This is because irrespective of complexity the obstacle definition in the graph environment is not effected as all points within the FOV need to be checked for occupancy. Oppositely for RRT, the larger the size and number of obstacles the higher the computational time required to check for collisions.

The success rate for the first three scenarios is over 90% for all percentage uncertainties for both algorithms considered with all three scenarios. A deterioration of approximately 5% with increase in uncertainty is visible only for RRT with A*'s success rate independent of uncertainty consideration. As remarked for path length and computational time with increase in buffer distance to obstacles the RRT is mainly effected as such buffer restricts prospective tree branches while for A* it does not effect obstacle definition within FOV, the most computational intensive part of the algorithm. For the Mixed case, a success rate between 52% and 70% and between 12% and 44% is recorded for A* and RRT, respectively. This shows that for the range of uncertainties considered for the Mixed case, the A* has double the chance of finding a feasible path from start to goal.

In comparison with the non uncertainty scenarios, an approximately 5% success rate deterioration is recorded for both algorithms for the first three scenarios for all the range of uncertainties considered. For the Mixed case, a success rate similar to the no uncertainty case for the same speed is recorded for both algorithms for all the range of uncertainties. As for the no uncertainty cases, the maximum intermediate time restriction is the main violation, especially in the Mixed case scenario for both algorithms. For A* a total time violation is also illustrated in less than 5% of the cases in the Mixed scenario. Oppositely, for RRT a number of No Path solutions are recorded (also less than 5%) for all scenarios increasing with increase in uncertainty. This results since the path to the intermediate goal point is constructed with the limitation that the path will be nearest to any obstacle by more than the maximum percentage uncertainty. When the actual uncertainty is added to the UAV position and the new intermediate path to a new intermediate goal point is being constructed, the movement of the obstacle may lead to the UAV being actually a smaller distance to the obstacle than the percentage allowable uncertainty. This will create a no path solution. As the uncertainty in UAV position buffer increases, the situations that can lead to this situation increases. For A*, this situation is less probable as in addition to this buffer distance another distance equivalent to half the distance between grid positions is added to avoid quantistion errors that could lead to erratic obstacle definitions.

In conclusion, both algorithms resulted in almost 100% success rate for the first three scenarios for all uncertainty values considered with RRT resulting in shorter path length and computational time with respect to A*. Both algorithms show an increase in path length and computational time with increase in uncertainty bounds with RRT showing the larger growth. For the Mixed case, A* is 2 times more successful than RRT for all uncertainty bounds with respect to RRT although A* constructed longer paths.

D. A* and RRT with uncertainty in obstacle position and orientation

Figure 5 illustrates the performance response of the A* and RRT algorithms with increase in obstacle uncertainty bounds. The uncertainty bound is calculated as a function of the size of the obstacles for 3D shapes like cubes. For 2D shapes including the V–obstacle and the two planes with windows constructed for the mixed case a bounding box the same shape as the obstacle is constructed. Therefore although for 3D shapes the number of planes remained the same (only increased in area with the consequence of increasing the enclosing volume) for 2D shapes the obstacle translated to a 3D obstacle with larger number of planes with increased area and unavailable volume. In this regard, for the V–obstacle a 10 plane, 3D obstacle enclosing the actual V–obstacle was constructed while for the planes with windows 24 planes instead of the original 4 per plane is required. Figure 6 graphically illustrates this explanation. This re–modelling of 2D obstacles increases complexity and therefore will have an effect on path planning performance.

Figure 5 (a) and (d) illustrate the path length for A* and RRT, respectively. The response is similar to the no uncertainty cases with the difference that no results are illustrated for the Mixed case scenario for the RRT algorithm since no successful runs were recorded for this case. In fact, the mean path length for A* increased by only 0.6%, 0.3%, 1.7% and decreased by 1.5% for the cube without and with rotation, V–obstacles and Mixed cases for the uncertainty with obstacle uncertainty with respect to the no uncertainty cases. Similarly, the same comparison for RRT the mean path length increased by only 0.3%, 0.2% and $<0.1\%$ for the first three scenarios. The small increase in the first three scenarios is attributed to the relative small increase in obstacle volume occupation. For the Mixed case, the decrease results due to a reduction of more than 50% of the obstacle uncertainty case with respect to the no uncertainty cases. With lower success

rate the easier paths are successful.

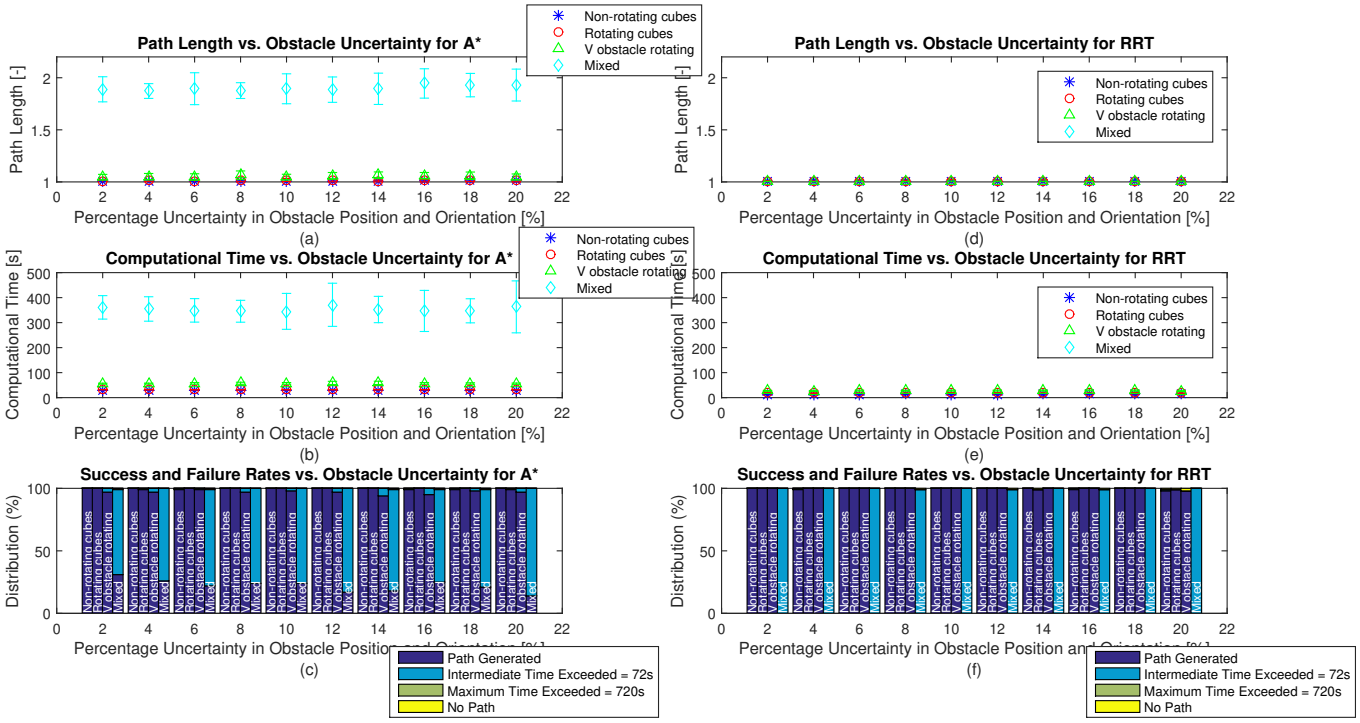

Figure 5. Performance parameters vs. Uncertainty in obstacle position and orientation: (a) Path Length for A*, (b) Computational Time for A*, (c) Success and Failure rates for A*, (d) Path Length for RRT, (e) Computational Time for RRT and (f) Success and Failure rates for RRT for 100 iterates for each considered situation (obstacle uncertainty and scenario) with 95% confidence interval. ($res = 21, d_{s\_step} = 0.05, d_{int\_goal} = 0.4$ **(for Scenarios 1,2 and 3) and** $d_{int\_goal} = 0.6$ **(for Scenario 4),** $d_{factor} = 0.8$**,** $t_{iterate\_max} = 72s$ **and** $t_{path\_gen\_max} = 720s$**.**

In comparison with the UAV positional uncertainty cases a lower increase in path length results for all scenarios for both algorithms as the uncertainty increases. In fact, comparing the path length at 20% with respect to 2% uncertainty an increase of 0.2%, 0.2%, 0.2% and 2.2% results for the non-rotating and rotating cube, V–obstacle and Mixed cases, respectively for the A* algorithm. A similar analysis for RRT showed an increase of <0.1%, 0.4% and 0.1% for the first three scenarios, respectively. For both algorithms, the variance is invariant with increase in obstacle uncertainty. Therefore, it can be concluded that the inclusion of obstacle uncertainty bounds have minimal effect on path length in the first three scenarios for both algorithms mainly due to the low occupation and also for the Mixed case using the A* algorithm.

The computational time results illustrated in Figures 5 (b) and (e) show that the cube with no rotation case exhibits the fastest time followed by the rotating cube, V–obstacle and Mixed scenarios for both algorithms. This order is different for both algorithms to both the no uncertainty cases and the uncertainty in UAV position test cases. In fact, for A* the computational time decreases by 2.34 and 2.33 times for the cube without and with rotation, respectively and increased by 3.72 and 1.49 times for the V–obstacle and Mixed scenarios, respectively for the obstacle uncertainty case with respect to the no uncertainty cases. A similar comparison for RRT shows that the computational time increased by 23.6%, 26.3% and 12.9 times for the first three scenarios, respectively.

The analysis shows that with the increase in effective inaccessible volume of the cubes, A* required less computational time while RRT required more time with respect to the no uncertainty case. Adding uncertainty bounds around obstacle makes it more difficult to construct a path as the environment is more restrictive. This explains why RRT requires more time to construct tree branches to find a path from start to goal. For A*, the increase in the number of inaccessible grid positions will not increase the environment grid definition time as explained earlier and will make it easier to find a path, if possible, since fewer amount of free nodes are available.

For the V–obstacle case both algorithms experienced an increase with RRT showing the larger increase. The inclusion of obstacle uncertainty has changed the V–obstacle from a 2D shape to a 3D shape. This

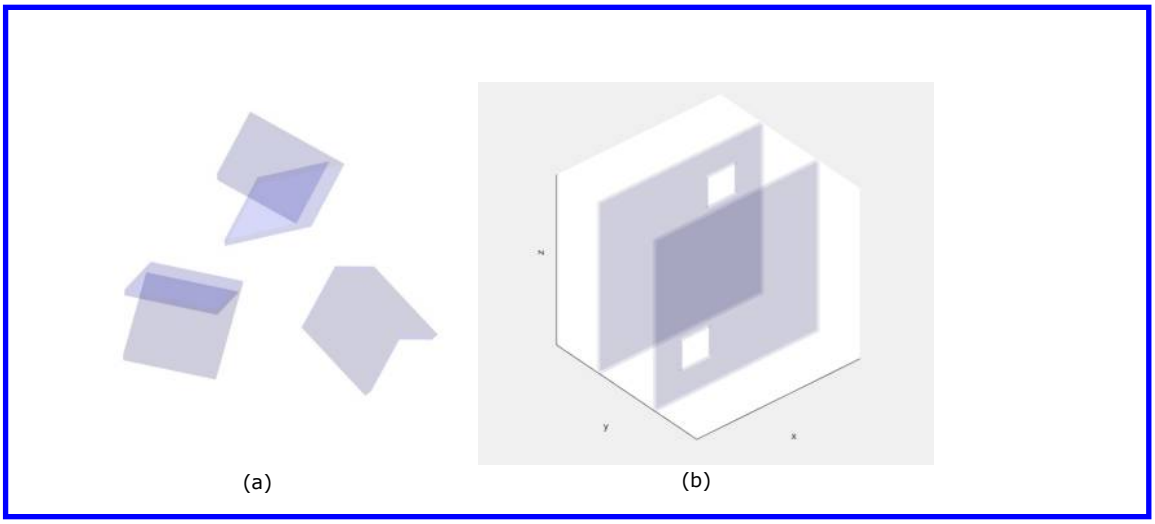

Figure 6. Two Dimensional objects modelled with uncertainty in obstacle position and orientation (20% test case): (a) V–obstacles (zoomed) and (b) Planes with windows constructed in Mixed Scenario.

increases computational demand to define the grid environment for A* since the grid definition sub–algorithm need to check and assign inaccessible grid points found internally within the obstacle. For RRT, the V–obstacle restricted the environment making it more difficult to construct tree branches. For the Mixed case scenario, the environment is more restrictive resulting in fewer options of tree branch construction, leading to a 0% success rate. For A*, the increase in computational time is attributed to the increase in grid definition time due to the change of 2D to 3D obstacles for the V–obstacles and planes.

Although the RRT experienced the higher increase in computational time, as for the non uncertainty situation, the RRT algorithm constructed the path in less time than the A* algorithm for the first three scenarios, implying that A*'s time consumption in environmental quantisation is more time consuming and path construction than RRT's approach even with the inclusion of uncertainty. This shows that the RRT algorithm remains more computationally efficient with respect to A* for simple scenarios with the inclusion of obstacle uncertainty in real–time.

Comparing the effect on computational time for obstacle uncertainty with respect to UAV positional uncertainty for A* show a minor decrease of 2.1%, 1.6% and a relatively larger increase of 20.9 times and 71.0% increase for the cube without and with rotation, the V–obstacle and Mixed case scenarios, respectively. This results since the increase of the cube size will increase the number of inaccessible grid positions for the obstacle uncertainty case remaining the same size for the positional UAv uncertainty. For the V–obstacle and Mixed cases the 2D to 3D shift in obstacle modelling for the obstacle uncertainty case is the reason for the increase with respect to the UAV positional uncertainty case in which the V–obstacles and planes remains 2D. A similar analysis for RRT shows a 6.3%, 15.9% and 11.4 times increase for the first three scenarios, respectively when comparing the mean computational time with obstacle uncertainty with respect to UAV positional uncertainty. Obstacle uncertainty makes the environment more restrictive due to increase in available volume resulting in larger computational demand requirement especially for the V–obstacle case.

The success rates for both algorithms illustrated in Figures 5 (c) and (f) show that a close to 100% success rate is recorded for both algorithm for the first three scenarios with a major drop for the Mixed case scenario for A* and 0% success rate for RRT. This shows that for the first 3 cases the success rate is indifferent for both algorithms in the range of uncertainty considered. For complex cases A* outperforms the RRT algorithm. The decrease in success rate as obstacle uncertainty increases is illustrated in the Mixed case for A* with a drop from 30% to 14% at 2% and 20% obstacle uncertainty, respectively. This is not shown for the other tests since the allocated time is either too high (First 3 scenarios) or too low (Mixed case, RRT). In fact, the maximum intermediate time violation is the major cause for unsuccessful runs.

In comparison with the no uncertainty cases, for A* no difference in success rate is recorded for the cube cases with a minor drop from 99% to an average of 96.9% in the V–obstacle due to the increased volume occupation of the V–obstacle a major drop from 69% to 22.2% for the Mixed case. The latter case includes both planes and V–obstacles that changed from 2D to 3D obstacles effectively increasing complexity. A similar analysis for RRT shows that for the first three scenarios the mean success rate with obstacle uncertainty is larger than 99.5% as opposed to the 100% with no uncertainty. This implies that the time restrictions are too large for these cases. For the Mixed case a drop from 30% to 0% is recorded.

In comparison with UAV positional uncertainty, overall results show that obstacle uncertainty deteriorates

success rate more than UAV positional uncertainty for the whole range of uncertainties considered for the Mixed cases with a less than 2% difference for the first three cases for both algorithms. For A*, a difference of less than 1% is recorded for the first 3 scenarios and a drop from 62.7% to 22.2% for the Mixed case for UAV positional and obstacle uncertainty, respectively. Similarly for RRT, a difference of less than 2% is recorded for the first 3 scenarios with a drop from 26% to 0% in mean success rate for the Mixed case.

In conclusion, the result show that a larger deterioration than the UAV positional uncertainty results for the obstacle uncertainty especially for RRT mainly for the V–obstacles and Mixed cases in terms of path length, computational time and success rate.

E. A* and RRT with uncertainty in obstacle position and orientation and UAV position

Figure 7 illustrates the performance response of the A* and RRT algorithms with the combined increase of obstacle position and orientation and UAV position uncertainties. The modelling of these uncertainties is as described in the previous two sub–sections and the scope of this analysis is to analyse the combined effect of these two unrelated uncertainties on the path planning performance of both algorithms at a predetermined speed.

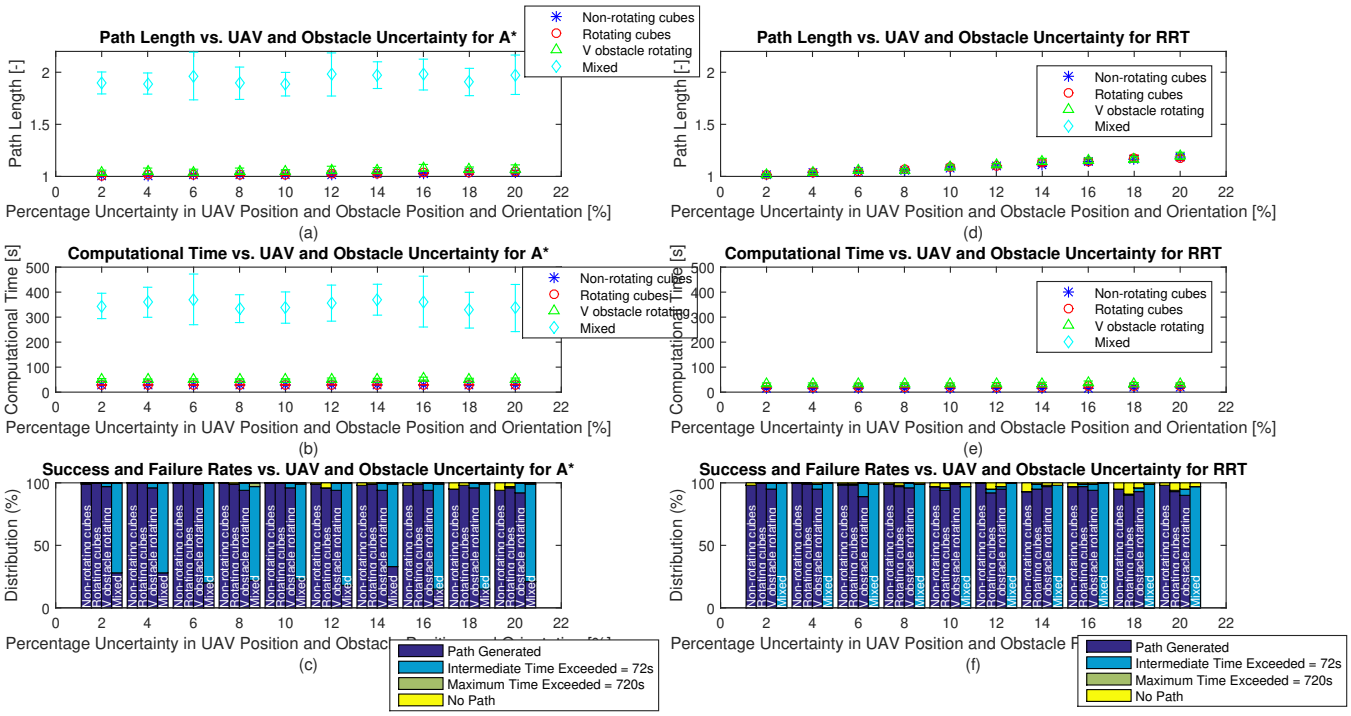

Figure 7. Performance parameters vs. Uncertainty in obstacle position and orientation and UAV position: (a) Path Length for A*, (b) Computational Time for A*, (c) Success and Failure rates for A*, (d) Path Length for RRT, (e) Computational Time for RRT and (f) Success and Failure rates for RRT for 100 iterates for each considered situation (obstacle and UAV uncertainty and scenario) with 95% confidence interval. ($res = 21, d_{s\_step} = 0.05, d_{int\_goal} = 0.4$ **(for Scenarios 1,2 and 3) and** $d_{int\_goal} = 0.6$ **(for Scenario 4),** $d_{factor} = 0.8$**,** $t_{iterate\_max} = 72s$ **and** $t_{path\_gen\_max} = 720s$**.**

Figures 7 (a) and (d) illustrate the path length for A* and RRT, respectively. The response in path length is a combination of the results of Figures 4 (a) and (d) and Figures 5 (a) and (d). For both A* and RRT algorithms an increase in path length results with increase in uncertainty with the major increase shown for RRT. For both algorithms the cube without rotation case produced the shortest path followed by the cube with rotation, V–obstacle and Mixed scenarios. Path length increases by 3.3%, 3.4%, 3.3% and 4.2% for the cube without and with rotation, V–obstacle and Mixed case scenarios, respectively for the A* algorithm as uncertainty increases from 2% to 20%. Similarly for RRT, an increase in path length of 16.7%, 15.4% and 17.8% for the first three scenarios, respectively as uncertainty increases from 2% to 20%. For the Mixed case in case of the RRT algorithm a 0% success rate is recorded as in the obstacle uncertainty test. This mainly results due to the larger increase in path length for RRT with increase in uncertainty. The RRT algorithm constructed shorter average paths of 7.2%, 7.2% and 4.4% with respect to A* for the first three

scenarios, respectively.

In comparison with the no uncertainty case, A* results show an average increase in path length of 1.8%, 1.6%, 1.9% and 0.2% for the cube without and with rotation, V–obstacle and Mixed case scenarios, respectively. The minor increase for the Mixed case is attributed to the lower success rate (>50%) and therefore the best performing paths are successful lowering the average path length. The UAV positional uncertainty tests result in an increase of 1.8%, 1.7%, 1.2% and 2.7% while the obstacle uncertainty result in 0.6%, 0.3%, 1.7% increase and 1.5% decrease with respect to the no uncertainty cases for the scenarios defined earlier, respectively. Analysis of these results show that both uncertainty types contribute to path length increase with UAV positional uncertainty having the predominant effect. Although the increase in obstacle size and buffer distance from UAV are equal, UAV positional uncertainty is added at each intermediate UAV position irrespective of whether an obstacle is in the vicinity or not. For the first three cases where the environment is mainly empty the deviations due to obstacles occur in few situations while deviations in UAV positional uncertainty occur at each intermediate UAV position. This explains the predominant effect of the UAV positional uncertainty results. For the Mixed case, which introduces a deviation from obstacle uncertainty at each intermediate UAV position due to the high obstacle density, results cannot be directly compared due to different success rates for the uncertainty cases considered.

Similarly for RRT, a comparison with the no uncertainty cases show an average increase in path length of 9.1%, 9.4% and 10.2% for the first three scenarios, respectively. The UAV positional uncertainty tests result in an increase of 9.2%, 9.1% and 46.6% while for obstacle uncertainty an increase of 0.3%, 0.2% and <0.1% is recorded for the first three scenarios, respectively with respect to the no uncertainty test case. As for A*, the major increase is recorded due to UAV positional uncertainty with obstacle uncertainty adding a low share to path length increase for the same reason described for A*. The difference for the V–obstacle scenario is attributed to the lower success rate for the combined uncertainty cases.

Figures 7 (b) and (e) illustrate the computational response time for the A* and RRT algorithms, respectively. The cube without rotation is the fastest scenario followed by the cube with rotation, V–obstacle and Mixed case scenarios (if success rate is not 0%) for both algorithms for all the uncertainty range considered. This order is different from the no uncertainty and UAV positional uncertainty tests and in line with the obstacle uncertainty test cases. The computational time comparison for A* at 2% and 20% uncertainty in obstacle and UAV position uncertainty result in a 4.4%, 6.2%, 2.2% increase and 2.4% decrease for the non–rotating cube, rotating cube, V–obstacle and Mixed case scenarios, respectively for 20% uncertainty with respect to 2% case. The decrease in Mixed case is attributed to the decreasing success rate. A similar analysis for RRT shows an increase of 35.1%, 27.9% and 7.6% for the first three scenarios implying that RRT's computational demand is more effected by uncertainty in comparison with A*. But RRT remains faster than A* for the first three scenarios by 74.8%, 33.9% and 53.6%, respectively mainly because of the time consuming grid definition of the environment.

A* results for combined obstacle and UAV positional uncertainties with respect to the no uncertainty case show an average decrease in computational time by 2.51 and 2.50 times and an increase of 3.38 and 1.48 times for the cube without and with rotation, V–obstacle and Mixed case scenarios, respectively. The decrease in the cube cases is mainly attributed to the reduced number of accessible grid positions making it faster to find a path, if possible. The shift from 2D to 3D obstacles in the V–obstacle and planes (Mixed case) increases the computational time to define inaccessible grid positions residing within obstacle bounds. Furthermore, the UAV positional uncertainty tests result in a decrease of 2.29, 2.29, 5.60 and 1.15 times while the obstacle uncertainty results in 2.34 and 2.33 times decrease and a 3.72 and 1.49 increase with respect to the no uncertainty cases for the scenarios defined earlier, respectively. This analysis shows that in terms of computational time obstacle uncertainty is predominant for the V–obstacle and Mixed case since the environment grid definition is predominately time consuming in 3D obstacles.

Similarly for RRT, a comparison with the no uncertainty cases show an average increase in computational time of 47.7%, 51.8% and 15.8 times for the first three scenarios, respectively. The UAV positional uncertainty test results in an increase of 16.3%, 8.9% and 13.1% while for obstacle uncertainty an increase of 23.6%, 26.3% and 12.9 times for the first three scenarios, respectively with respect to no uncertainty cases. As both positional and obstacle uncertainties increase computational time their effect in restricting path construction is summed up in the combined test case.

The success rates for both algorithms illustrated in Figures 7 (c) and (f) show a success rate near to 100% for the first three scenarios for both algorithms for the range of uncertainties considered with a major drop for A* and a drop to 0% for RRT for the Mixed case scenario in line with the obstacle uncertainty test

cases. As concluded for the obstacle uncertainty case, the success rate for the first three scenarios is the same for both algorithms with A* performing better than RRT in the Mixed case scenario. For A* the success rate drops by 5%, 4%, 5% and 7% for the cube without rotation, with rotation, V–obstacle and Mixed case, respectively from 2% to 20% uncertainties. For the same analysis, the RRT results in a success rate drop of 1%, 6%, 5% and 0% (0% success rate). Therefore it can be concluded that success rate drops with increase in uncertainty for both algorithms.

As previously, the maximum intermediate time violation is the major cause of unsuccessful runs with 78 tests out of 4000 resulting in No Path solution only for RRT with the number increasing with increase in percentage uncertainty. This violation only occurs for RRT since the planner does not incorporate the half the distance between grid position as in A* and therefore the movement of an obstacle towards the UAV can result in a collision, as explained earlier. This risk will improve path length but is dangerous and can lead to a collision especially in the presence of uncertainty.

Comparing the success rates for the uncertainty in obstacle and position with respect to the no uncertainty test cases for A* show a decrease of 0.7%, 1.3%, 3.8% and 46.7% for the cube without rotation, with rotation, V–obstacle and Mixed case scenarios, respectively. Also, the UAV positional uncertainty test show a drop <7% for all scenarios and for obstacle uncertainty a drop <3% for the first three scenarios with a major drop of 46.8% for the Mixed case scenario all with respect to no uncertainty cases. This analysis show that success rate is hindered mainly by obstacle uncertainty especially in the Mixed case since in this situation the environment is already obstacle dense without increase in the obstacle bounds. In general, bounds will increase the inaccessible grid points making it more difficult to find a solution while UAV positional uncertainty will only limit the minimum distance to the obstacle which is already buffered by half the distance between grid positions.

A similar analysis for RRT show a drop in success rate of 2.5%, 4.5%, 5.7% and 30% for the combined obstacle and UAV positional uncertainty with respect to the no uncertainty test case for the same speed for the cube without rotation, with rotation, V–obstacles and Mixed case scenarios, respectively. The UAV positional uncertainty test case results in a drop of 2.1%, 2.0%, 1.5% and 4% for the same scenarios as previously while for the obstacle uncertainty test case results in a drop <1% (First three scenarios) and 30% for the Mixed case with respect to the no uncertainty test cases. The analysis shows that, as opposed to A*, both uncertainties contribute to the drop in success rate owing to the nature of the RRT algorithm that both uncertainties will restrict tree branch construction increasing the path planning time with the consequence increasing unsuccessful runs.

In conclusion, with the inclusion of both obstacle and UAV positional uncertainties path planning performance further deteriorates, especially for RRT, with respect to the consideration of individual uncertainties.

F. Conclusion

This section presented, compared and analysed the real–time path planning performance of both A* and RRT algorithms in 4 different scenarios with and without uncertainty in obstacles and UAV position. Results show that the inclusion of uncertainties deteriorates path length, computational time and success rate with the larger deterioration exhibited for the RRT algorithm. Overall, RRT performed better in the cube and V–obstacle scenarios in terms of path length and computational time with A* performing better in complex scenarios. Both uncertainties deteriorates path planning performance differently. The inclusion of both uncertainties at the same time further hinders performance especially for RRT. In conclusion, this analysis confirms that uncertainties shall be considered in path planning as their effect especially in complex scenarios will determine the safety and success of the mission.

VI. Conclusion and Future Work

This paper analysed the path planning performance of the A* and RRT algorithms in 3D real–time UAV path planning in different complexity scenarios with moving obstacles in the presence of uncertainties in UAV position and obstacle position and orientation. Literature identified the need to consider uncertainty sources in UAV path planning owing to their effect on constraints and disturbances within which a UAV must safely operate. In this regard, two different uncertainties, the UAV position and obstacle position and orientation, that incorporated all identified uncertainty sources for the considered UAV, were quantified and modelled using bounded shapes. The UAV model, path planner parameters and four different complexity

scenarios were defined in view of real UAV models and the environment into which these are expected to operate. The path length, computational time and success rate were the performance measures considered, as uncertainty was varied between 2% and 20%.

Results show that both types of uncertainty deteriorate path planning performance of both A* and RRT algorithms for all scenarios considered with RRT exhibiting the larger effect on performance due to both types of uncertainties. RRT results in the fastest and shortest paths with approximately the same success rate as A* (>95%) for the cube and V–obstacle scenarios deteriorating significantly to even 0% success rate for the Mixed scenario. In latter case A* performs better. The combination of both types of uncertainty into the same test further deteriorates performance especially for RRT. Also owing to RRT's ability to shorter path nearer to obstacles with respect to A* results show that RRT has a higher risk of collision than A*. The results show that both algorithms can be applied in low obstacle density environments with moving obstacles in real–time path planning in the presence of uncertainty. In complex scenarios more time is required, especially for RRT, for comparable success rates. Finally, this work shows that 3D real–time path planning in different obstacle density, moving obstacle environments in the presence of uncertainty is possible.

Future enhancement shall include the analysis of the effects of other parameters including look–ahead distance, distance to travel per iterate and allocated time on the performance of both path planning algorithms. A future work is the implementation of the developed 3D real–time path planning algorithms to configure a real UAV for autonomous 3D UAV navigation in an indoor obstacle–rich environment.

References

[1]International Civil Aviation Organisation, "Global Air Traffic Management Operational Concept", *Doc. 9854*, AN/458, Ed. 1, pp. 1–82, 2005.

[2]International Civil Aviation Organisation, "Unmanned Aircraft Systems (UAS)", *Cir. 328*, AN/190, pp. 1–54, 2011.

[3]Boskovic, J. D., Knoebel, N., Moshtagh, N. and Larson, G.L., "Collaborative Mission Planning & Autonomous Control Technology (CoMPACT) System Employing Swarms of UAVs", *AIAA Guidance, Navigation and Control Conference*, Chicago, IL, 10–13 Aug., 2009, pp. 1–24.

[4]Goerzen, C., Kong, Z. and Mettler, B. "A Survey of Motion Planning Algorithms from the Perspective of Autonomous UAV Guidance", *Journal of Intelligent & Robotic Systems*, Vol. 57, pp. 65—100, 2010.

[5]Dadkhah, N. and Mettler, B., 'Survey of Motion Planning Literature in the Presence of Uncertainty: Considerations for UAV Guidance", *Journal of Intelligent & Robotic Systems*, Vol. 65, pp. 233—246, 2012.

[6]Vanegas, F. and Gonzalez, L. F., "Uncertainty based online planning for UAV target finding in cluttered and GPS-denied environments", *IEEE Aerospace Conference*, Big Sky, MN, 5–12 Mar., 2016, pp. 1–9.

[7]Chakrabarty, A. and Langelaan, J. W., "Energy maps for long–range path planning for small-and micro–uavs", *AIAA Guidance, Navigation and Control Conference*, Chicago, IL, 10–13 Aug., 2009, pp. 1–13.

[8]Benenson, R. Petti, S., Fraichard, T. and Parent, M., "Integrating Perception and Planning for Autonomous Navigation of Urban Vehicles," *IEEE/RSJ International Conference on Intelligent Robots and Systems*, Beijing, China, 9–15 Oct. 2006, pp. 98–104.

[9]Yao, P., Wang, H. and Su, Z., "Real-time path planning of unmanned aerial vehicle for target tracking and obstacle avoidance in complex dynamic environment," *Aerospace Science and Technology*, Vol. 47, pp. 269–279, 2015.

[10]Zammit, C. and van Kampen, E. J., "3D real–time path planning of UAVs in dynamic environments", *AIAA Guidance, Navigation and Control Conference*, AIAA SciTech Forum, Kissimmee, FL, 8–12 Jan., 2021.

[11]Zammit, C. and van Kampen, E. J., "Comparison between A* and RRT Algorithms for UAV Path Planning", *AIAA Guidance, Navigation and Control Conference*, AIAA SciTech Forum, Kissimmee, FL, 8–12 Jan., 2018, pp. 1–23.

[12]Zammit, C. and van Kampen, E. J., "Advancements for A* and RRT in 3D path planning of UAVs", *AIAA Guidance, Navigation and Control Conference*, AIAA SciTech Forum, San Diego, CA, 7–11 Jan., 2019, pp. 1–17.

[13]Zammit, C. and van Kampen, E. J., "Comparison of A* and RRT in real–time 3D path planning of UAVs", *AIAA Guidance, Navigation and Control Conference*, AIAA SciTech Forum, Kissimmee, FL, 6–10 Jan., 2020.

[14]Kim, Y., Gu, D.-W., Postlethwaite, I., "Real-time path planning with limited information for autonomous unmanned air vehicles", *Automatica*, Vol. 44, No. 3, pp. 696—712, 2008.

[15]Hsu, D., Kindel R., Latombe J. C., Rock, S., "Randomized kinodynamic motion planning with moving obstacles", *International Journal Robotics Research*, Vol. 21, No. 3, pp. 233—255, 2002.

[16]Cui, J.–H., Wei, R.–X., Liu, Z.–C. and Zhou, K., "UAV Motion Strategies in Uncertain Dynamic Environments: A Path Planning Method Based on Q–Learning Strategy", *Applied Sciences*, Vol. 8, No. 11, pp. 2169, 2018.

[17]LaValle, S. M. and Sharma, R. "A Framework for Motion Planning in Stochastic Environments: Modeling and Analysis", *IEEE lnternational Conference on Robotics and Automation*, Nagoya, Japan, 21–27, May 1995, pp. 3057–3062, 1995.

[18]Hoy, M., Matveev, A. S. and Savkin, A. V., "Algorithms for collision–free navigation of mobile robots in complex cluttered environments: a survey", *Robotica*, Vol. 33, No. 4, pp. 463–497, 2014.

[19]Liao, F., Lai, S., Hu, Y., Cui, J., Wang, J. L., Teo, R. and Lin, F. "3D Motion Planning for UAVs in GPS–Denied Unknown Forest Environment", *IEEE Intelligent Vehicles Symposium*, Gothenburg, Sweden, 19–22, Jun. 2016, pp. 246–251.

[20]Vanegas, F., Campbell, D., Roy, N., Gaston, K. J. and Gonzalez, L. F., "UAV tracking and following a ground target under motion and localisation uncertainty", *IEEE Aerospace Conference*, Big Sky, MN, 4–11 Mar., 2017, pp. 1–10.

[21]Achtelik, M. W., Lynen, S., Weiss, S., Chli, M. and Siegwart, R., "Motion- and Uncertainty-aware Path Planning for Micro Aerial Vehicles", *Journal of Field Robotics*, Vol. 31, No. 4, pp. 676–698, 2014.

[22]Prentice, S. and Roy, N. "The Belief Roadmap: Efficient Planning in Belief Space by Factoring the Covariance" *The International Journal of Robotics Research*, Vol. 28, No. 11-12, pp. 1448–1465, 2009.

[23]He, R., Bachrach, A. and Roy, N., "Efficient planning under uncertainty for a target-tracking micro-aerial vehicle", *IEEE International Conference on Robotics and Automation*, Anchorage, AK, 3–7, May 2010, pp. 1–8.

[24]Florence, P. R."Integrated Perception and Control at High Speed", Master Dissertation, Massachusetts Institute of Technology, Feb. 2017.

[25]Lihua, Z., Xianghong, C. and Fuh–Gwo, Y. "A 3D collision avoidance strategy for UAV with physical constraints" *Measurement*, Vol. 77, pp. 40–49, 2016.

[26]Kothari, M. and Postlethwaite, I., "A Probabilistically Robust Path Planning Algorithm for UAVs Using Rapidly-Exploring Random Trees", *Journal of Intelligent & Robotic Systems*, Vol. 71, pp. 231–253, 2013.

[27]Rathbun, D., Kragelund, S., Pongpunwattana, A. and Capozzi, B., "An evolution based path planning algorithm for autonomous motion of a UAV through uncertain environments", *Digital Avionics Systems Conference*, Irvine, CA, 27–31, Oct. 2002, pp. 8.D.2-1–8.D.2-12.

[28]LaValle, S. M. and Sharma, R. "A Framework for Motion Planning in Stochastic Environments: Applications and Computational Issues ", *IEEE lnternational Conference on Robotics and Automation*, Nagoya, Japan, 21–27, May 1995, pp. 3063–3068.

[29]LaValle, S. M., *Planning algorithms*, Cambridge: Cambridge university press, 2006.

[30]Majumdar, A. and Tedrake, R. "Funnel libraries for real-time robust feedback motion planning", *The International Journal of Robotics Research*, Vol. 36, No. 8, pp. 947–982 2017.

[31]Moore, J., Cory, R. and Tedrake, R. "Robust post-stall perching with a simple fixed-wing glider using LQR–Trees", *Bioinspiration & Biomimetics Journal*, Vol. 9, No. 2, pp. 1–24 2014.

[32]Shah, S. K, Pahlajani, C. D., Lacock, N. A. and Tanner, H. G. "Stochastic receding horizon control for robots with probabilistic state constraints", *International Conference on Robotics and Automation (ICRA)*, St. Paul, MN, 14–18, May, 2012, pp. 2893–2898.

[33]Blackmore, L., Ono, M. and Williams, B. C. "Chance-constrained optimal path planning with obstacles", *IEEE Transactions on Robotics*, Vol. 27, No. 6, pp. 1094–1080, 2011.

[34]Luders, B., Kothari, M. and How, J.P. "Chance constrained RRT for probabilistic robustness to environmental uncertainty", *AIAA Guidance, Navigation, and Control Conference and Exhibit*, Toronto, Ontario, Canada, 02–05 Aug. 2010, pp. 1–21.

[35]Page, L. A. and Sanderson, A. C. "A path-space search algorithm for motion planning with uncertainties", *IEEE International Symposium on Assembly and Task Planning*, Pittsburgh, PA, 2–5, Aug. 1995, pp. 334–340.

[36]Lazanas, A. and Latombe, J.-C. "Landmark-based robot navigation", *Algorithmica*, Vol. 13, No. 5, pp. 472–501, 1995.

[37]Larson, J., Bruch, M. and Ebken, J. "Autonomous navigation and obstacle avoidance for unmanned surface vehicles", *Defense and Security Symposium, SPIE conference*, Kissimmee, Orlando, FL, 17—21, Apr. 2006, pp. 1–12.

[38]Yang, L., QI, J., Jiang, Z., Song, D., Han, J. and Xiao, J. "Guiding Attraction based Random Tree Path Planning under Uncertainty: Dedicate for UAV", *International Conference on Mechatronics and Automation*, Tianjin, China, 3—6, Aug. 2014, pp. 1182–1187.

[39]Pepy, R. and Lambert, A. "Safe Path Planning in an Uncertain–Configuration Space using RRT", *IEEE International Conference on Intelligent Robots and Systems*, Beijing, China, 9–15 Oct. 2006, pp. 5376–5381.

[40]van den Berg, J., Wilkie, D., Guy, S. J., Niethammer, M. and Manocha, D. "Lqg-obstacles: Feedback Control with Collision Avoidance for Mobile Robots with Motion and Sensing Uncertainty", *IEEE International Conference on Robotics and Automation*, St. Paul, MN, 4–18 May 2012, pp. 346–353.

[41]Zeng, Z., Lammas, A., Sammut, K., He, F. and Tang, Y. "Shell space decomposition based path planning for AUVs operating in a variable environment", *Ocean Engineering*, Vol. 91, pp. 181–195, 2014.

[42]Gonzalez, J. P. and Stentz, A., "Planning with uncertainty in position an optimal and efficient planner", *IEEE/RSJ International Conference on Intelligent Robots and Systems*, Edmonton, Alta., Canada, 2–6 Aug. 2005, pp. 1–8.

[43]Wen, N., Xiaohong, S., Ma, P., Zhao, L. and Zhang, Y. "Online UAV path planning in uncertain and hostile environments", *International Journal of Machine Learning and Cybernetics*, Vol. 8, pp. 469–487, 2017.

[44]Daftry, S., Zeng, S., Khan, A., Dey, D., Melik-Barkhudarov, N., Bagnell, J. A. and Hebert, M. "Robust Monocular Flight in Cluttered Outdoor Environments", *ArXiv*, Vol. 1604.04779, pp. 1–10, 2016.

[45]Matthies, L., Brockers, R., Kuwata, Y. and Weiss, S. "Stereo vision-based obstacle avoidance for micro air vehicles using disparity space", *IEEE International Conference on Robotics and Automation (ICRA)*, Hong Kong, China, 31 May–7 Jun. 2014, pp. 3242–3249.

[46]Liu, S., Watterson, M., Tang, S. and Kumar, V. "High speed navigation for quadrotors with limited onboard sensing.", *IEEE International Conference on Robotics and Automation (ICRA)*, Stockholm, Sweden, 16-21 May 2016, pp. 1484-3249.

[47]Kuwata, Y., Karaman, S., Teo, J., Frazzoli, E., How, J. and Fiore, G. "Real–Time Motion Planning With Applications to Autonomous Urban Driving", *IEEE Transactions on Control Systems Technology*, Vol. 17, No. 5, pp. 1105–1118, 2009.

[48]Fulgenzi, C., Tay, C., Spalanzani, A. and Laugier, C. "Probabilistic navigation in dynamic environment using rapidly-exploring random trees and Gaussian processes", *IEEE International Conference on Intelligent Robots and Systems*, Nice, France, 22–26 Sep. 2008, pp. 1056—1062.

[49]Kewlani, G., Ishigami, G. and Iagnemma, K. "Stochastic mobility–based path planning in uncertain environments", *IEEE International Conference on Intelligent Robots and Systems*, St. Louis, MO, 11–15 Oct. 2009, pp. 1183–1189.

[50]Melchior, N.A. and Simmons, R. "Particle RRT for path planning with uncertainty", *IEEE International Conference on Robotics and Automation*, Rome, Italy, 10–14 Apr. 2007, pp. 1617–1624.

[51]Aoude, G. S., Joseph, J., Roy, N. and How, J.P. "Mobile Agent Trajectory Prediction using Bayesian Nonparametric Reachability Trees", *Infotech@ Aerospace*, St. Louis, MO, 29–31 Mar. 2011, pp. 1587–1593.

[52]Papadimitriou, C. H. and Tsitsiklis, J. N. "The Complexity of Markov Decision Processes", *Mathematics of Operations Research*, Vol. 12, No. 3, pp. 441–450, 1987.

[53]Thrun, S., Burgard, W. and Fox, D. 'Probabilistic Robotics', Massachusetts: MIT Press, 2005.

[54]Pineau, J., Gordon, G. and Thrun, S. "Anytime Point–Based Approximations for Large POMDPs", *Jounal of Artificial Intelligence Research*, Vol. 27, No. 1, pp. 335–380, 2006.

[55]Utkin, V. I. 'liding Modes in Control Optimization', Berlin: Springer–Verlag, 1992.

[56]Shah, M. Z., Samar, R. and Bhatti, A. I. "Guidance of Air Vehicles: A Sliding Mode Approach", *IEEE Transactions on control system technology*, Vol. 23, No. 1, pp. 231–244, 2015.

[57]Yang, L., Qi, J., Song, D., Xiao, J., Han, J. and Xia, Y. "Survey of Robot 3D Path Planning Algorithms", *Journal of Control Science and Engineering*, Vol. 2016, pp. 1–22, 2016.

[58]Culligan, K., Valenti, M. Kuwata, Y. and How, J. P. "Three dimensional flight experiments using on-line mixed-integer linear programming trajectory optimization", *American Control Conference*, New York, NY, 9–13 Jul. 2007, pp. 5322–5327.

[59]Masehian, E. and Habibi, G. "Robot path planning in 3D space using binary integer programming", *International Journal of Mechanical System Science and Engineering*, Vol. 23, pp. 26–31, 2007.

[60]Anderson, S., J., Peters, S. C., Pilutti, T. E. and Iagnemma, K. "An optimal-control-based framework for trajectory planning, threat assessment, and semi-autonomous control of passenger vehicles in hazard avoidance Scenarios", *International Journal of Vehicle Autonomous Systems*, Vol. 8, No. 2–4, pp. 190–216, 2010.

[61]Connolly, C. I. "Harmonic functions and collision probabilities", *International Journal of Robotics Research*, Vol. 16, No. 4, pp. 497–507, 1997.

[62]Lazanas, A. and Latombe, J. C. "Motion planning with uncertainty: a landmark approach", *Artificial Intelligence*, Vol. 76, No. 1–2, pp. 287–317, 1995.

[63]Zengin, U. and Dogan, A., J. C. "Probabilistic trajectory planning for UAVs in dynamic environments", *AIAA "Unmanned Unlimited" Technical Conference, Workshop and Exhibit*, 20–23 Sep., 2004, Chicago, IL, pp. 1–12.

[64]Thrun, S., Diel, M. and Hahnel, D. "Scan alignment and 3–D surface modelling with a helicopter platform", *International Conference on Field and Service Robotics*, Yamanashi, Japan, 14–16 Jul. 2003, pp. 1–6.

[65]Thrun, S. and Montemerlo, M. "The graph slam algorithm with applications to large-scale mapping of urban structures", *International Journal of Robotics Research*, Vol. 25, No. 5–6, pp. 403–429, 2006.

[66]Kuwata, Y., Schouwenaars, T., Richards, A. and How, J. "Robust constrained receding horizon control for trajectory planning", *AIAA Guidance, Navigation, and Control Conference*, San Francisco, CA, 15–18 Aug. 2005, pp. 1–12.

[67]Schouwenaars, T., Mettler, B., Feron, E. and How, J. P. "Robust Motion Planning Using a Maneuver Automaton with Built-in Uncertainties", *American Control Conference*, Denver, Co, 4–6 Jun. 2003, pp. 2211–2216.

[68]Frazzoli, E. 'Robust Hybrid Control for Autonomous Vehicle Motion Planning', Ph. D. thesis, MIT, June 2001.

[69]Gonzàlez, D., P*èrez*, J., Milanès, V., and Nashashibi, F., "A Review of Motion Planning Techniques for Automated Vehicles", *IEEE Transactions on Intelligent Transportation Systems*, Vol. 17, No. 4, pp. 1135–1145, 2016.

[70]Ghandi, S. and Masehian, E., "Review and taxonomies of assembly and disassembly path planning problems and approaches", *CAD Computer Aided Design*, Vol. 67–68, No. October, pp. 58–86, 2015.

[71]Tseng, F. H., Liang, T. T. and Lee, C. H. Chou, L. D. and Chao, H., "A Star Search Algorithm for Civil UAV Path Planning with 3G Communication", *10th International Conference on Intelligent Information Hiding and Multimedia Signal Processing (IIH–MSP)*, Kitakyushu, Japan, 27–29 Aug. 2014, pp. 942–945.

[72]Hart, P. E., Nilsson, N. J. and Raphael, B., "A Formal Basis for the Heuristic Determination of Minimum Cost Paths", *IEEE Transactions on Systems Science and Cybernetics*, Vol. 4, No. 3, pp. 100–107, 1968.

[73]Short, A., Pan, Z., Larkin, Z. and van Duin, S. "Recent Progress on Sampling Based Dynamic Motion Planning Algorithms", *IEEE International Conference on Advanced Intelligent Mechatronics (AIM)*, Alberta, Canada, Jul. 2016, pp. 1305–1311.

[74]LaValle S. M. "Probabilistic roadmaps for path planning in high–dimensional configuration spaces", *IEEE Transactions on Robotics and Automation*, Vol. 12, No. 14, pp. 566–580, 1996.

[75]Lavalle S. M. and Kuffner J. J., "Randomized kinodynamic planning", *International Journal of Robotics Research*, Vol. 20, No. 3, pp. 378–400, 2001.

[76]LaValle, S. M. and Kuffner, J. J. "Randomized kinodynamic planning", *Proceedings of the IEEE International Conference on Robotics and Automation*, Detroit, MI, 10–15 May 1999, pp. 473–479.

[77]Devaurs, D., Siméon, T. and Cortés, J. "Optimal Path Planning in Complex Cost Spaces With Sampling–Based Algorithms", *IEEE Transactions on Automation Science and Engineering*, Institute of Electrical and Electronics Engineers, 2015.

[78]Geraerts, R. and Overmars, M. "Creating high–quality paths for motion planning", *International Journal of Robotics Research*, Vol. 26, No. 8, pp. 845–863, 2007.

[79]Sujit, P. B., and Ghose, D., "Search by UAVs with Flight Time Constraints using Game Theoretical Models," *AIAA Guidance, Navigation and Control Conference*, San Francisco, CA, 15–19 Aug. 2005, pp. 1–11.

[80]Bethke, B., Bertuccelli, L. How, J. P., "Experimental Demonstration of MDP–Based Planning with Model Uncertainty," *AIAA Guidance, Navigation and Control Conference*, Honolulu, HI, 18–21 Aug. 2008, pp. 1–22.

[81]Bollino, K., Lewis, L. R., Sekhavat, P. and Ross, I. M., "Pseudospectral Optimal Control: A Clear Road for Autonomous Intelligent Path Planning," *AIAA Infotech Aerospace Conference and Exhibit*, Rohnert Park, CA, 7–10 May 2007, pp. 1–14.